NATIONAL TRANSPORTATION SAFETY BOARD
Office of Research and Engineering
Materials Laboratory Division
Washington, D.C. 20594

February 1, 2017

MATERIALS LABORATORY FACTUAL REPORT Report No. 17-001

A. ACCIDENT INFORMATION

Place : New Martinsville, West Virginia
Date : August 27, 2016
Vehicle : AXLX 1702 Liquid Chlorine Tank Car
NTSB No. : DCA16SH002
Investigator : Paul Stancil, RPH-20

B. COMPONENTS EXAMINED

AXLX 1702 Liquid Chlorine Tank Car, DOT 105J500W

C. DETAILS OF THE EXAMINATION

AXLX 1702 was initially examined at the Natrium, West Virginia facilities of Axiall Corporation (now Westlake Axiall) on September 1, 2016. The car was further examined and samples were removed the following week, see upper view of figure 1. Initial examinations and testing of the removed samples began September 20 in the NTSB Materials Laboratory. Parties to the investigation (at the time), FRA and Axiall were present during the on-scene and initial laboratory examinations of the car and pieces.

1. AXLX 1702 General

The tank car was manufactured by ACF Industries in 1979 to meet DOT-105A500W[1] standards. The tank of the car (heads and rings) was made from non-normalized American Association of Railroads (AAR) TC-128 Grade B[2] carbon steel with a specified ultimate tensile strength between 81,000 psi and 101,000 psi, a minimum 50,000 psi yield strength and at least 16% elongation in an 8 inch grip length. The as-manufactured minimum thickness for the heads and shell was 0.7751 inch.

The pressure tank was constructed with two elliptically shaped heads and five rings all joined by submerged arc welds. Rings were numbered, 1 through 5, from the B end[3] of the car. The sump and manway were located in ring 3. The tank was attached to the running gear through ACF 200 design stub sills. The design utilizes cradle pads welded to the tank to transfer running loads from the stub sills through the tank. The cradle pads extend from the respective tank heads across most of the adjacent two rings of the tank, see illustration in lower view of figure 1. The tank was covered with 4 inches of fiber

[1] 49 CFR Part179 Subpart C “Specifications for Pressure Tank Car Tanks (DOT-105, 109, 112, 114 and 120)
[2] AAR Manual of Standards and Recommended Practices M-1002 Appendix M
[3] Designated by the location of the brake wheel. The opposite end of the car is denoted the A end.

thermal insulation and an outer steel jacket. Unless otherwise noted in this report, directions and numbering references are viewed from the B end of the car looking toward the A end.

a. Previous Known Repairs

AXLX 1702 was shopped in 2016 as part of Axiall's fleet maintenance program. An inspection at this time found numerous corrosion pits in the lower interior section of the tank. The pits were subsequently ground and repaired by weld overlay. The accident occurred during the first load following the repairs.

The tank had also undergone various exterior repairs at various times during 2010 and at various facilities. These included crack repairs by grinding and welding[4] at the inboard ends of the A and B end cradle pads, urethane foam insulation removal and replacement with fiber insulation and weld repairs of corrosion pits on the exterior top of the tank. The car was also fully rejacketed .

2. Initial Inspections and Sample Removal

During the initial inspections of the car on September 1, portions of the jacket and insulation had been previously removed, shown in figure 2. Examinations of the tank through the removed portions revealed an approximately 42 inch long, mostly circumferential, crack in the 4th ring of the tank near the inboard end of the A end stub sill, as shown in the upper view of figure 3. The crack surfaces and surrounding area of the tank had been sprayed with a preservative compound[5] prior to NTSB examinations. Additional portions of the car jacket and appliances were removed at the direction of the Safety Board and the tank was again examined the following week. In addition, the jacket, insulation and appliances were removed from the area of the inboard end of the stub sill at the B end of the car.

The crack was located about 0.25 to 0.5 inch inboard of the A end stub sill cradle pad and ran circumferentially across the bottom of the tank. To the right (left in views), the crack ended near the right corner of the cradle pad and showed local yielding of the tank material. To the left, the crack ran partially up the side of the tank and split into two legs. One leg continuing circumferentially about 13 inches before arresting and the other leg turned horizontally toward the B end. This leg terminated at the fusion weld between the 4th and 3th rings. The crack faces were gapped apart about 0.25 inch at the bottom of the tank. However, the only visible yielding deformation was at the right end of the crack.

Different appearing welds were apparent at the inboard ends of both right and left cradle pad to tank welds, see green brackets lower view of figure 3. The different weld were consistent with manually applied shielded metal arc repair welds as documented in the 2010 repairs. On the right side, the repair weld was about 2.5 inches long and about 2 inches long on the left side of the cradle pad.

[4]AAR Manual of Standards and Recommended Practices M-1002. Appendix R Section 10.2. 10/2007
[5] Reported to be LPS 3, by ITW Pro Brands Tucker, GA

Photographic measurements at the end of the cradle pad prior to opening of the cracks found approximately 8.5 inches between the welds (indicated by blue arrow in the lower view of figure 3). Complying with the drawing[6] notation of “no weld 8” 2 PLCS” for the end of the cradle pads.

The tank outer surface surrounding the crack displayed general surface corrosion and numerous pits. The corrosion and pitting were also noted in locations remote to the crack. Some of the corrosion appears as severe deep pitting. In areas away from the crack, the exterior surface of the tank appeared to be cover with a light tan paint or primer.

The entire area of the crack including portions of both the 3rd and 4th rings were flame cut from the tank for further examination. In addition, an approximate 20 inch by 26 inch uncracked area was removed from the right side of the 4th ring for mechanical tests of the material.

Internal inspections of the tank were performed after the samples were removed. Multiple weld repairs and places where the surface had been abrasively ground were noted on the interior surface but no corrosion pitting was noted. The interior surface of the removed cracked section had 13 visible weld repairs. Of these, eight welds and 11 ground spots were noted in ring 4 and five repair welds and two ground spots were found in ring 3. Two weld repair areas were just inboard of but did not intersect the crack. The interior surface of the removed sample at the A end is displayed in upper view of figure 4. The lower view of figure 4 is marked and annotated to show the locations of the weld repairs and ground spots. In addition, the shape and location of the end of the cradle pad located on the opposite side is illustrated (dashed blue lines).

Using a straight edge, a deformation of the ring 4 was noted between the crack at the cradle pad and the ring 3 to 4 weld joint. In the approximate 11 inch distance, the interior surface was deformed downward approximately ½ inch. The circumferential extent of the deformation was not established. The measurement location for this deformation is denoted by the double green arrow in the lower view of figure 4.

Inspections of the interior surface also uncovered an area of heavy surface oxide (scale) near the right corner of the A end cradle pad, as shown in the two views of figure 5. The boundaries of the scaling were indistinct but estimated to be at least 12 inches in diameter and included the right side termination of the crack, denoted by the purple area in the lower view of figure 4. The scaling was indicative of high temperature exposure and later measured to be greater than 0.03 inch in thickness, as shown in figure 6.

The end of the cradle pad at the B end of the tank was also examined on-scene. Visual inspections did not reveal any obvious cracks. However, repair welds, similar to those noted at the A end, were noted at the inboard 2 to 3 inches of the cradle pad to tank welds. The entire end of the pad along with the surrounding tank material were removed by flame cuts for further examination. Two weld repair locations and 3 ground

[6] ACF Drawing “Attachments Welded Stub Sill U.F.” 2-C-2118, 9-3-86 last revision date.

spots were visible on the interior surface of the removed piece. The removed B end piece will be further discussed below.

3. A End Laboratory Examination

The A end crack was opened by band saw cuts (purple brackets) to near the ends of the crack and applying force to break the remaining ligaments, as show in figure 7. Features on the revealed crack faces (lower view figure 7) were consistent with brittle fracture propagation for the entire length of the crack. Chevron markings on the crack faces demonstrated that the crack initiated near the toe of the left hand repair weld bead, as shown in figure 7. Propagation was circumferentially away from the left weld. Progression to the right side arrested (dashed red line) near the right cradle pad repair weld, but did not intersect the weld or its apparent heat affected zone. Crack propagation to the left continued to propagate circumferentially before splitting into two legs with the longer portion turning toward the B end of the car and arresting in the fusion weld (dashed red line) connecting rings 3 and 4. The shorter leg of the crack (dashed yellow line) continued for a distance and arrested in the middle of the plate.

The crack area near the cradle pad and welds was further sectioned as indicated in figure 8. The removed pieces of crack were cleaned and the previously sprayed on corrosion preventative compound was removed by ultrasonic agitation in toluene. The sections containing the crack initiation are shown in figure 9. Closer inspection of the initiation area after cleaning uncovered a darker-colored elliptically-shaped region at the weld toe. The dark coloration and magnified appearance were consistent with an oxide layer. The elliptical region was oriented at about 45 degrees to the plate surface approximately bisecting the intersecting surfaces of the weld bead and the surface of the plate. The dark region was poorly defined but was estimated to be about 0.7 inch wide by about 0.2 inch deep.

The initiation region also roughly followed the curved shape of the toe of the weld as shown in figure 10. The lower view of figure 10 also shows the toe of the repair bead (outlined in yellow) projecting past the end of the cradle pad (dashed blue line) by almost 0.30 inch (double red arrow). The repair weld bead was about 0.76 inch wide at the end of the pad. Also note in the upper view that the exterior surface of the tanks exhibited extensive surface corrosion pits (green arrows).

The repair weld appeared to contain multiple weld beads that blended together for a relatively uniform surface. The weld bead also transitioned smoothly into the tank material with no apparent undercutting noted and only one weld spatter ball was visible.

As shown in figure 11, the right terminus of the crack (red arrow) did not intersect the right side cradle pad repair weld (outlined by the dashed yellow line) but rather arrested just inboard of the repair weld. The end of the crack exhibited significant bulk yielding deformation not seen at any other location along the crack. During opening of the crack, the repair weld was partially cut into but details remained showing that the repair weld was made of several beads that did not blend smoothly together. The B end of the weld partially wrapped around the corner of the cradle pad and exhibited poor

workmanship with a large undercut area at the end and adjacent large melt balls, see figure 12. The repair weld also visually exhibited surface-connected pores on the sides and lack of penetration at the end.

Opening the large crack also opened an oxide-covered preexisting crack through the repair weld. The preexisting weld crack measured about 0.6 inch wide and 0.3 inch deep is outlined in yellow in figure 12.

b. SEM

After extensive ultrasonic cleaning in detergent and alcohol, the inboard side (B side) of the crack initiation and surrounding areas were examined with a scanning electron microscope (SEM). At lower magnification, the initiation area displayed a woody fracture topography as shown in the upper view of figure 13. Closer viewing and Energy Dispersive Spectrographic Analysis (EDS) showed that the woody initiation region was covered by a heavy oxide layer that obscured and obliterated the fine fracture features.

Further SEM viewing away (approximately 1.5 inches) from the initiation area revealed a much flatter surface but also heavily oxidized with destruction of the fine fracture features.

c. Metallographic Sections

Four metallographic sections were cut near the fracture initiation area. The sections were numbered #1, #2, #3 and #4. Two additional specimens, #5 and #6, were prepared from unwelded areas to the right of the crack. The metallographic specimens are labeled and displayed in their relative positions in figure 14. For the sections through welds, the fusion and heat affected zone (HAZ) microstructures were, in general, consistent with low-carbon steel welds. Each section along with deviations and discontinuities are described below. All section were etched with 2% Nital[7] reagent.

Section #1, figure 15, was through one of the interior surface weld repairs near the fracture. The weld fusion zone and underlying HAZ were each about 0.09 inch deep. A microhardness traverse revealed a generally uniform hardness across the weld, HAZ and base metal as shown by the chart in figure 15. Hardness ranged from 91 to 100 HRB.

Section #2 was through the repair weld area just outboard (toward A end) of the crack initiation area on the left side of the cradle pad. As shown in figure 16, the repair weld contained multiple (possibly 5) beads with a large internal pore showing slag inclusions and a lack of fusion between two of the beads. The repair also contained two under bead cracks angling across the heat affect zone near the root of the weld. The cracks measured 0.094 inch and 0.109 inch deep. A third crack was present between the root pass fusion zone and HAZ measured 0.037 inch deep. The HAZ measured about 0.034 inch wide at the toe of the weld and slightly greater elsewhere. A microhardness

[7] 2% concentrated nitric acid in ethyl alcohol.

traverse revealed a generally uniform hardness across the weld, HAZ and base metal as shown by the chart in figure 16. Hardness ranged from 92 HRB to 25 HRC.

Metallographic section #3 was through the original manufacturing weld just outboard of the repair weld . As shown in figure 17, it appeared to be made with at least 2 beads and contained a small slag inclusion between them. The cap bead also had a small 0.03 inch surface crack. No undercutting was noted at the tank side toe of the weld and the heat affected zone measured about 0.03 inch at the tank side toe of the weld. A microhardness traverse revealed a generally uniform hardness across the weld, HAZ and base metal as shown by the chart in figure 17. Hardness ranged from 93 HRB to 24.5 HRC.

Section #4 showed the base microstructure of the tank material near the initiation area but away from any welds. The microstructure was mixed equiaxed pearlite and ferrite grains consistent with a low carbon steel, as shown in figure 18. The grain size was generally fine but with a mixture of larger and smaller sizes. The estimated average grain size of about 10[8]. The microstructure appeared uniform through the thickness of the tank plate with no obvious banding or segregation. The tank plate was also very clean with very few stringers noted.

Hardness of the tank material was measured by both direct HRB and microhardness indentations on sample #4. Both methods produced similar results with a combined average hardness of 93.7 HRB.

As indicated in figure 14, a longitudinal strip was cut from ring 4 of the tank about 6 inches to the right of the end of the crack. Metallurgical sections #5 and #6 were parallel to the rolling direction of the plate prepared from specimens at opposite ends of the strip. Section #5 was in the previously noted scaled area of the tank and section #6 located about 12 inches towards the A end was visually out of the oxidized area.

When etched with 2% Nital reagent, both specimens displayed clean microstructures similar to that described for sample #4 above. Sample #5, figure 19, exhibited more pearlite-pearlite banding compared to #6, figure 20. The grain size as measured by line intercept, as above, was slightly smaller for specimen #5 at 9.70 compared to 10.09 for #6. Average microhardness for #5 was 86.4 HRB while average hardness for #6 was 94.8 HRB.

Sample #5 from the scaled area also showed decarburization and scaling of both the interior and exterior surfaces. Generally, the decarburization was about 0.006 inch deep, as shown in figure 21. Sample #6 did not show any significant surface decarburization or significant oxidation.

[8] By software based on ASTM E112-12 Standard Test Methods for Determining Average Grain Size.

d. Surface Hardness

Following sectioning of the crack and A end welds, HRB hardness measurements were made on the tank material at several locations. At some locations, the hardness measurements were made directly on band saw cut surfaces, at other places the surfaces were ground or abrasively sawn prior to hardness measurement. Figure 22 shows the sectioning of ring 4 of the tank around the fracture initiation area and inboard end of the cradle pad.

To the right of the view (car left), hardness on three tank pieces located both inboard and outboard of the crack averaged 91.3 HRB, 93.7 HRB and 91.2 respectively. The two long pieces to the left of the view (car right) were through the previously noted scaled area and direct hardness measurements were made along the band saw cut surfaces. The measured hardness along the circumferential piece (horizontal in the view) was relatively uniform from end to end and averaged 81.4 HRB. The adjacent square piece also displayed generally uniform hardness values that averaged 84.6 HRB. However the longitudinal strip (shown vertically in figure 22) showed two distinct hardness regions. Hardness of the 6 to 7 inches toward the B end of the car averaged 81.4 HRB. Hardness of the 6 to 7 inches at the A end of the strip were markedly harder averaging 93.1 HRB. The transition between the two region was abrupt going from an 83.7 HRB value to 92.4 HRB in about one inch. Metallographic sections #5 and #6 were made from each end of this strip, microhardness measurements showed a similar distinct difference between the ends of the strip (see section above).

e. Tank Thickness

The tank thickness was measured at various locations in ring #4 throughout the examinations. Measurements were made using either micrometers or calipers. Local thickness varied with corrosion pitting on the exterior surfaces of the tank. The tank thickness as specified on the original build engineering drawings was a minimum of 0.7751 inch. Axiall maintenance instructions specify a minimum allowable thickness of 0.7438 inch at the tank bottom for car AXLX 1702.

Thickness measurements along the crack near the initiation area from right to left were: 0.745 inch, 0.763 inch, 0.773 inch, and 0.773 inch. Thickness measurements were also taken in 1” increments along the yellow bracket sections in figure 22. From the B end to the A end they were 0.725 inch, 0.705 inch, 0.7665 inch, 0.7570 inch, 0.7675 inch, 0.7705 inch, 0.7565 inch, 0.7725 inch, 0.7690 inch, 0.7690 inch, 0.7705 inch and 0.7755 inch. The first two measurements were within the scaled area with the scale removed and were less than the specified minimum. Additional measurements were made on the tank inboard and outboard of the crack initiation. All measurements were greater than minimum specified thickness and ranged from 0.7580 inch to 0.7730 inch, see purple brackets in figure 22.

f. Mechanical Tests and Chemistry

Mechanical testing and chemical analysis of the #4 ring material was conducted at Lehigh Testing Laboratories, Inc. Tests included tensile tests, and Charpy impact tests per ASTM 370-15[9], in both the longitudinal and transverse directions[10] of the plate[11]. Three 8-inch tensile tests were performed in both directions. The results for ultimate, and yield strengths and elongation in 8 inches met the minimum requirements for AAR TC-128 grade B steel[12]. The chemical composition of ring #4 was also analyzed. Except for minor deviations in the percentages of sulfur, aluminum and boron, the ring met the pre 2015 product analysis[13] requirements for TC-128 grade B. Carbon equivalent[14] was calculated to be 0.4197.

Although not required at the time of original tank manufacture, Charpy impact tests were also conducted at temperatures between -100 F and 200 F. Three specimens were broken at each temperature. The results are plotted and shown in figure 23. Effective August 1, 2005[15], TC128 steel used for pressure tanks must be Charpy impact tested transverse to the rolling direction and must meet a minimum of 15 ft-lb at -30 ºF. For "low-temperature service" cars, the plates must be 15 ft-lb or more at -50 ºF. As shown, material from ring 4 of AXLX 1702 would not have met the present requirement in either direction.

4. B End Laboratory Examination

As previously noted and shown in figure 24, the inboard end of the cradle pad and adjacent tank shell from the B end of the car was also cut out of the tank for additional laboratory examinations. Visual examination found two to three inch long repair welds (green brackets), similar to those at the A end on both sides of the inboard end of the cradle pad.

Initial inspections found that the repair welds on both sides of the cradle pad slightly turned the inboard corners of the pad as shown in the lower view of figure 24. Photographic measurements at the end of the cradle pad found slightly less than 7 inches between the welds (blue double arrow). Not meeting the drawing[16] notation of "no weld 8" 2 PLCS" for the end of the cradle pads.

[9] ASTM International, Standard Test Methods and Definitions for Mechanical Testing of Steel Products, 2015.
[10] The longitudinal and transverse property directions are related to the rolling direction of the plate. Longitudinal is the direction of plate rolling that for the ring is circumferential. Transverse is across the rolling direction or along the length of the tank.
[11] Full results are contained in 17-001, Appendix A.
[12] Shown in Table M.3 of AAR Manual M-1002 (11/2014).
[13] Shown in Table M.2 of AAR Manual M-1002 (11/2014).
[14] Using CE = C + (Mn/6) + ((Cr + Mo + V)/5) + ((Ni + Cu)/15).
[15] Section 2.2.1.2 of AAR Manual M-1002 (11/2014).
[16] ACF Drawing "Attachments Welded Stub Sill U.F." 2-C-2118, 9-3-86 last revision date.

The outer surfaces of the B end sample were cleaned by baking soda blasting, see lower views of figure 24. The repair welds displayed poor workmanship with significant undercutting into the tank, uneven bead sizes, surface porosity and weld spatter.

After additional grit blast cleaning of the exterior surfaces, the left side repair weld area was subjected to several nondestructive testing methods using nonstandard techniques[17] (NDT) including radiography, angle beam ultrasonic, visible dye penetrant and wet and dry magnetic particle testing. The magnetic particle techniques both detected crack indications in an undercut area at the inboard tip of the repair weld as displayed in figure 25. Visual examinations at low magnifications after testing did not visually confirm cracking.

g. Metallographic Sections

Six metallographic specimens were prepared through the original and repair welds of the B-end piece. These included a transverse section through the original and repair welds on each side and longitudinal sections through the repair welds at their inboard tips, as shown in figure 26. The longitudinal section through the left repair weld was through the location of the previously noted NDT crack indication as indicated by yellow dashed lines in figure 25. The sections were numbered B10 through B15 and shown in figures 27 to 32. Each section was etched with 2% Nital and all showed microstructures consistent with multi-pass fusion welds in low carbon steel.

Sample B10 was through the original manufacturing weld and the right side of the B end cradle pad to tank joint, shown in figure 27. The microstructure was consistent with a two or three pass weld with no discontinuities noted in the section.

Figure 28 displays section B11 through the right side repair weld. As shown, the weld had a ~0.1 inch long crack at the tank side toe and some lack of fusion at the root. The toe crack was wholly contained within the HAZ. The weld also had a sharp toe at the pad side. A microhardness traverse across the weld, HAZ and into the tank base metal showed a somewhat harder HAZ compared to the adjacent areas.

Section B12 was a longitudinal section through the right side repair weld and is displayed in figure 29. The repair weld contained an oxide-filled toe-crack and lack of fusion as indicated.

The manufacturer’s original weld, section B13, on the left side of the cradle pad is shown in cross section by figure 30. The weld joint was a two-pass weld and showed a small slag inclusion between passes and a small area of lack of fusion at the root. A microhardness traverse across the weld, HAZ and into the tank base metal showed a harder HAZ compared to the adjacent areas.

[17] Testing performed as a group function at Testing Technologies Inc., Woodbridge, Virginia.

A transverse section, B14, through the left side repair weld on the B end revealed a multi-bead weld with several slag inclusions larger than 0.1 inch, as shown in figure 31. A microhardness traverse across the weld, HAZ and into the tank base metal showed a large HAZ that was both harder and softer than the adjacent weld and base metal.

Figure 32 shows the longitudinal section, B15, through the area of the NDT crack indication confirming the presence of an oxide filled crack at the tank side toe of the repair weld. Significant undercutting is also visible. The section also revealed another crack at the root of the weld in the HAZ and an area lacking fusion between the weld and the cradle pad. Both cracks were contained within the HAZ and did not penetrate into the unaffected base metal. The root crack and lack of fusion are shown in figure 33 along with a graph of a microhardness traverse across the weld, HAZ and base metal.

h. Surface Hardness

Surface hardness measurements using the Rockwell B scale (HRB) were made directly on the abrasively-cut surfaces of the B end tank material at two locations on the left side and one on the right side. The left side measurements averaged 93.9 HRB and 91.7 HRB. The single right side locations averaged 92.6 HRB. The hardness values had an aggregate average of 92.9 HRB.

Joe Epperson
Senior Metallurgist

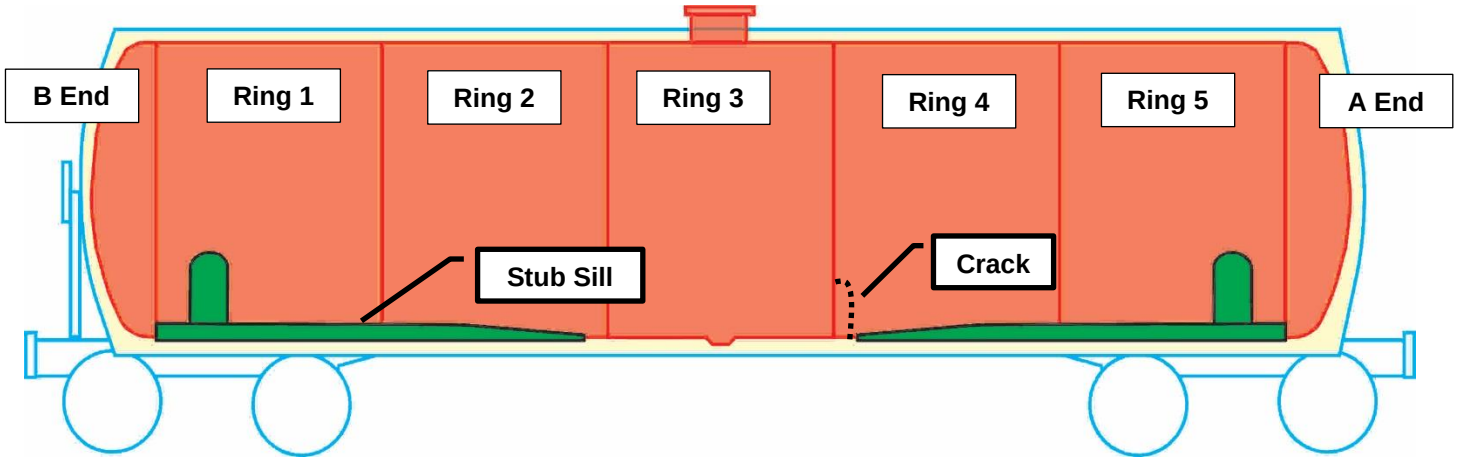

Figure 1. A view of the left side of AXLX 1702 from the A end. Lower view illustrates the general construction of the car and particularly the tank with the B end at the left. Stub sills are in green with the approximate crack location on opposite side of car indicated. Tank ring identifications are also denoted, Ring 1 thru Ring 5.

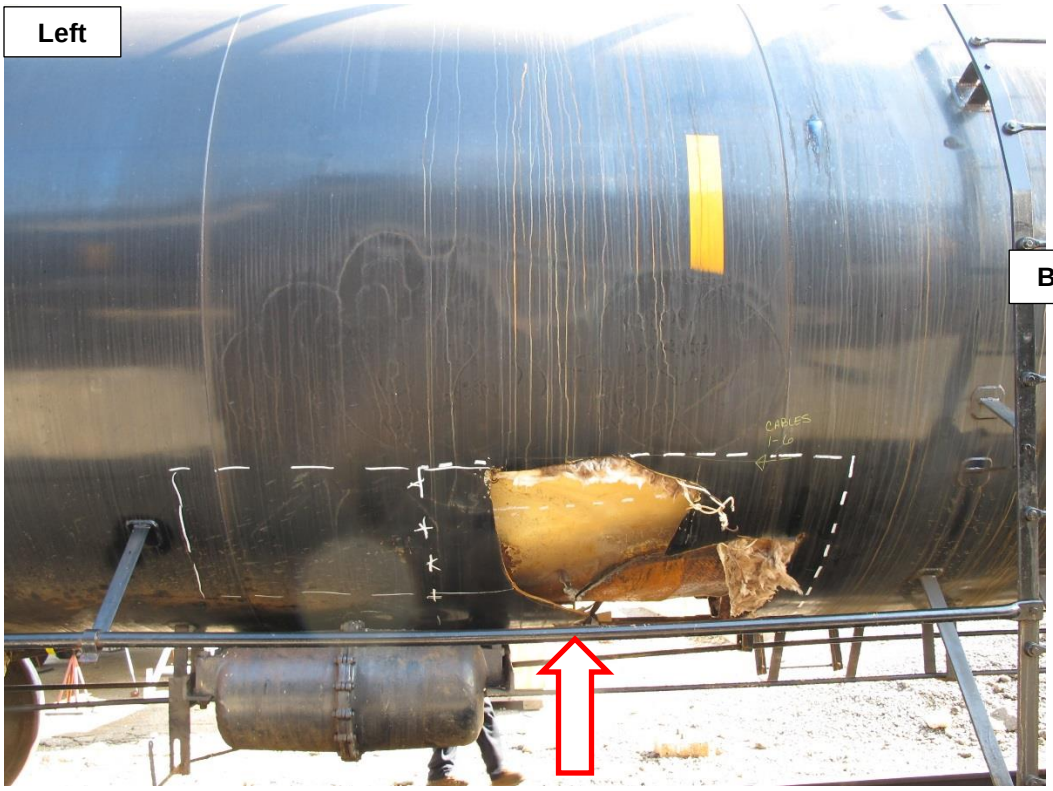

Figure 2. The leak area (red arrows) as viewed on September 1, 2016 with portions jacket and insulation already removed.

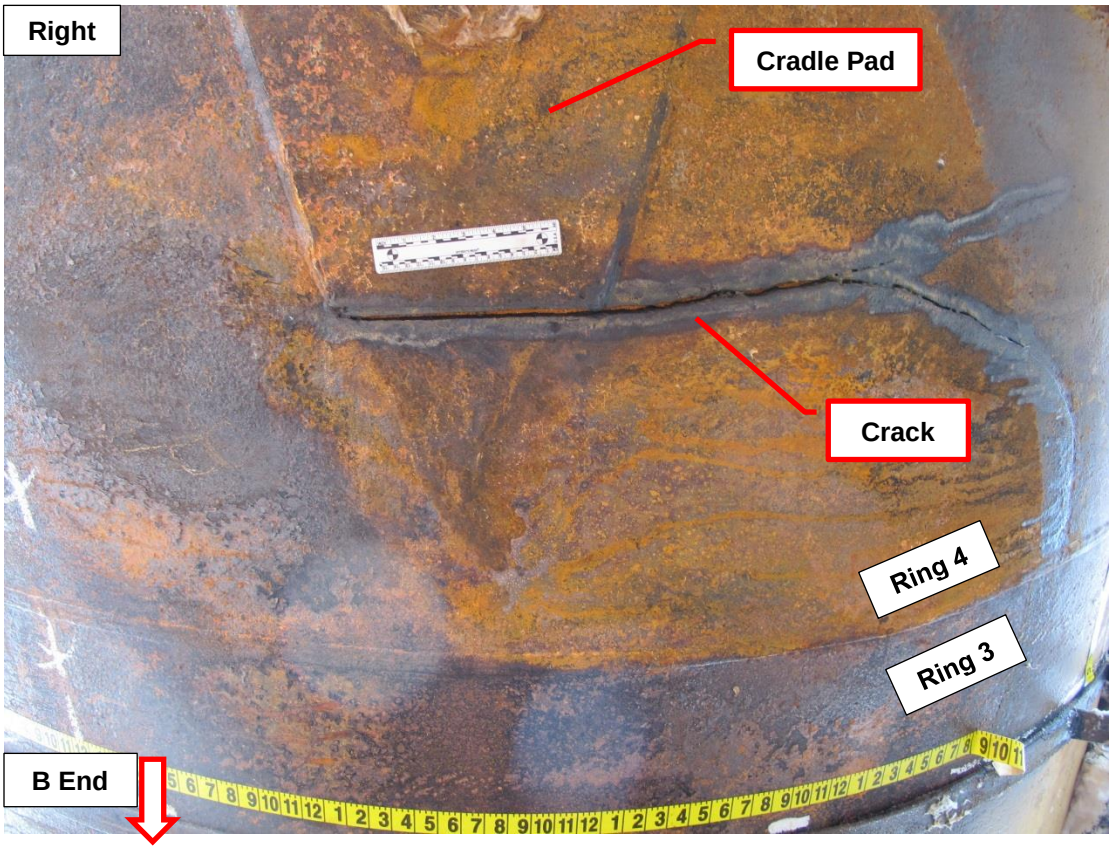

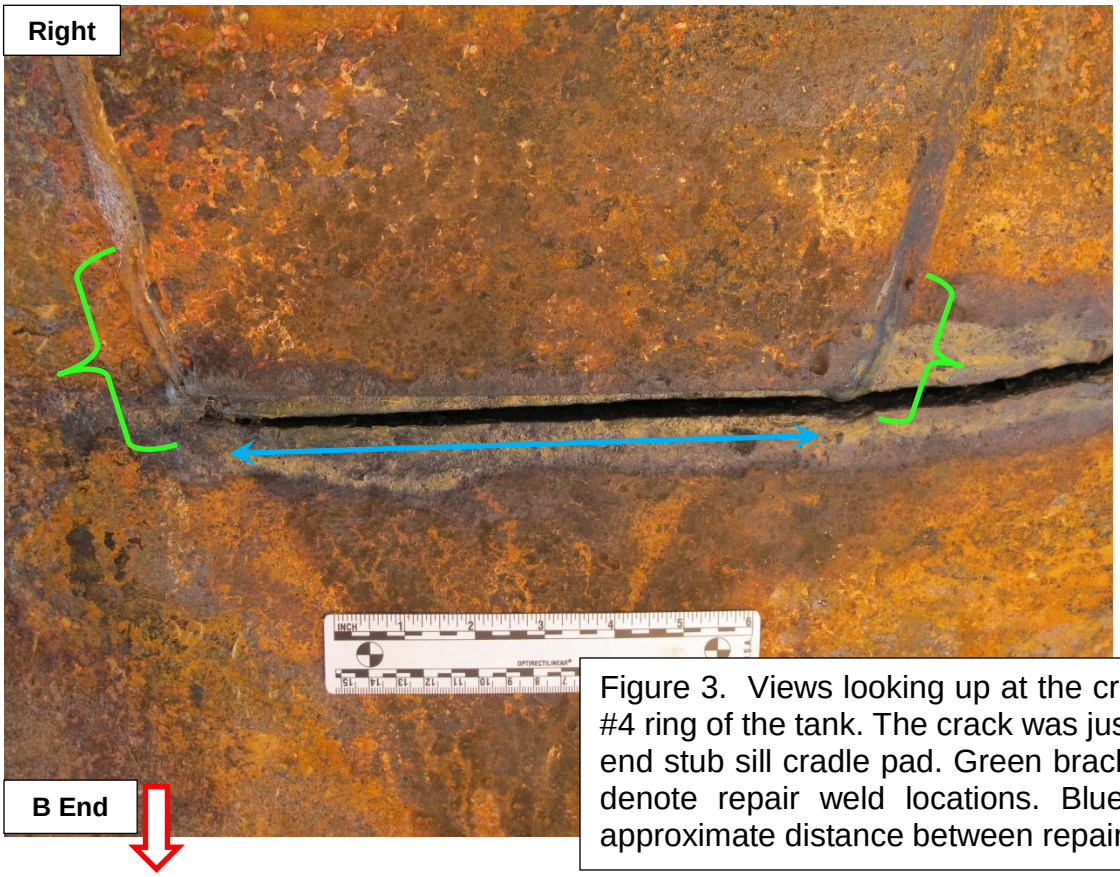

Figure 3. Views looking up at the cracked area of the #4 ring of the tank. The crack was just inboard of the A end stub sill cradle pad. Green brackets in lower view denote repair weld locations. Blue arrow indicates approximate distance between repair welds.

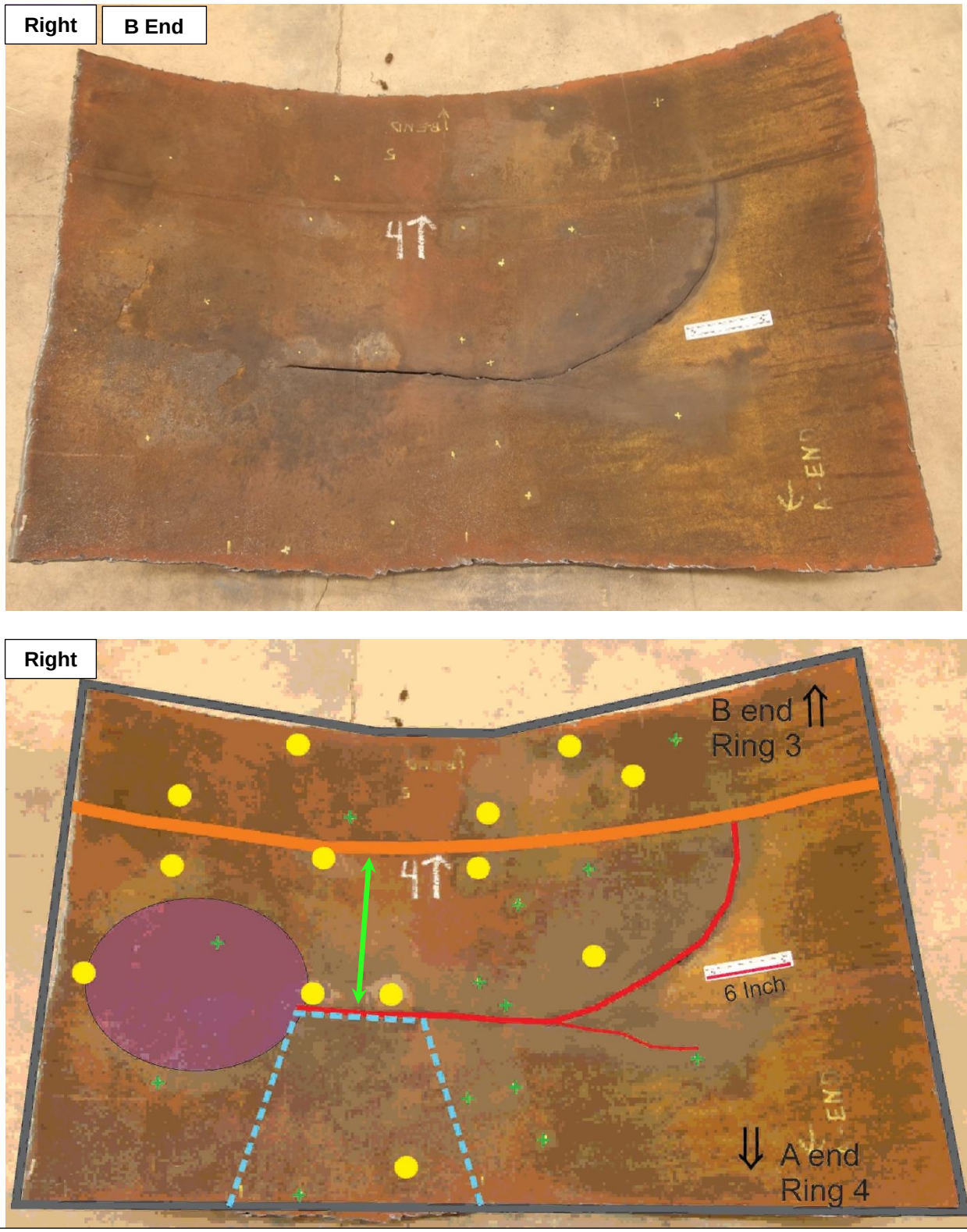

Figure 4. Upper view shows the interior tank surface of the removed A end section containing the crack. The lower view is annotated showing the crack location, red line, the weld repair spots, yellow circles, the ground spots green plus marks and the manufacturing weld between ring 3 and ring 4, wide orange line. The shape of the cradle pad is also indicated by the dashed blue line. The purple oval on the left indicates the visible scaling on the interior surface. (see figure 5)

Figure 5. Two views of the surface scaling on the interior of the tank. Broken edges of oxide scale are visible.

Figure 6. At top is a closer view of the surface scale where it has partially flaked off a cut piece of the tank. The lower view shows the scale in cross section with thickness measurements.

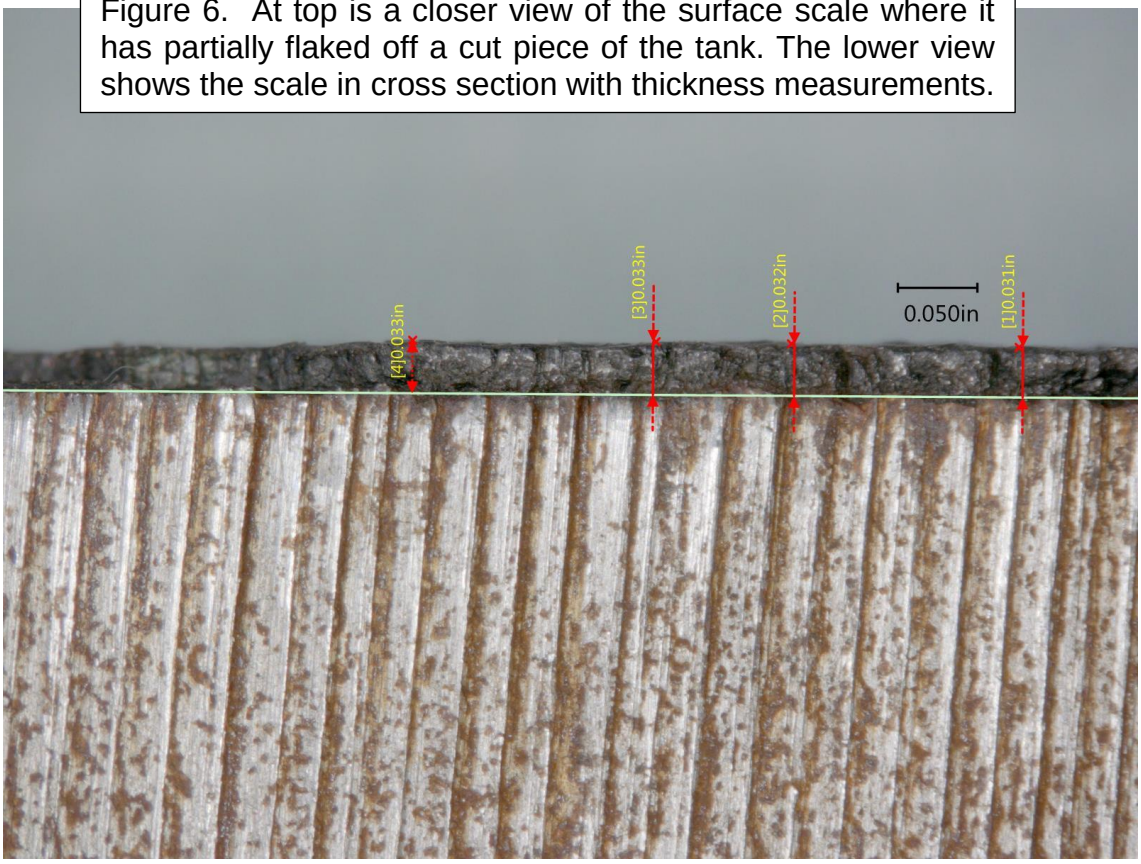

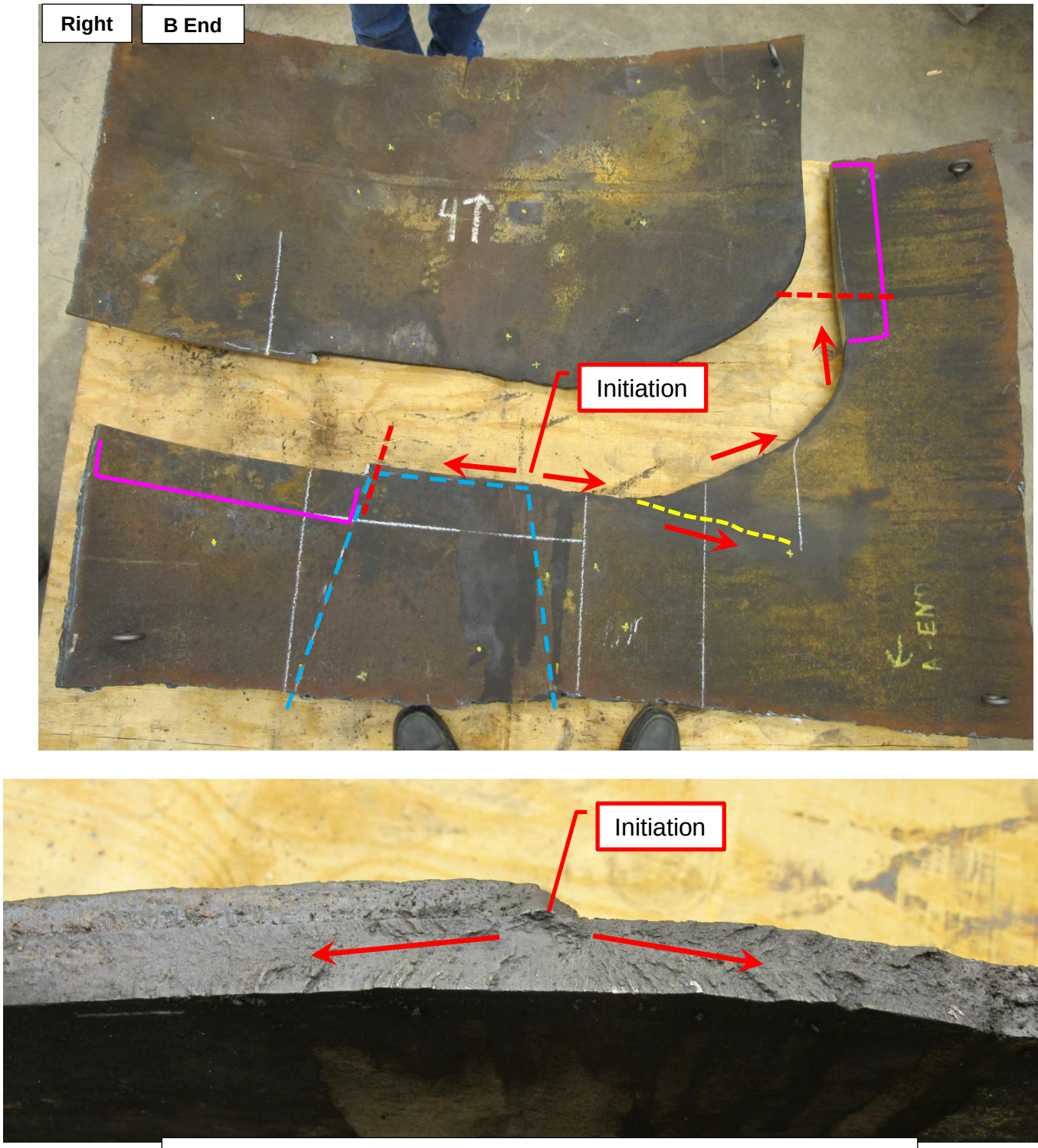

Figure 7. Top view shows the interior surface of the tank after the crack was opened by saw cut (purple brackets). The initiation area at the left repair weld of the cradle pad (outlined as dashed blue) is shown with the propagation directions indicated by red arrows to the crack termini at the dashed red lines. Lower view shows brittle propagation away (red arrows) from the initiation at the repair weld.

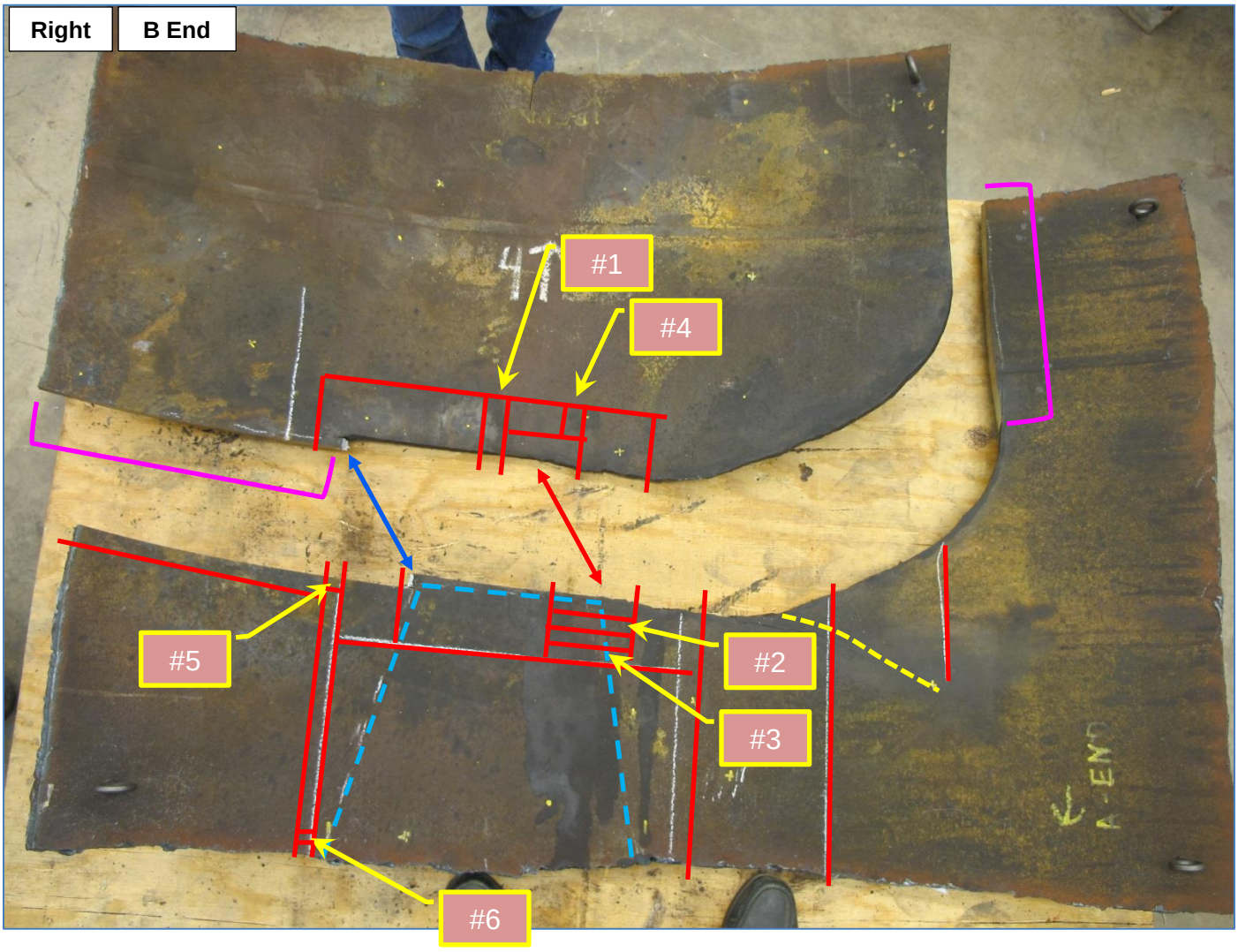

Figure 8. The opened crack with the initial saw cuts at the purple brackets and subsequent sectioning lines indicated by red lines. Double headed arrows denote mating locations on the two pieces of tank. Locations of metallographic sections #1 thru #6 are also indicated. Dashed blue lines denote the location of the cradle pad on the opposite of the shell.

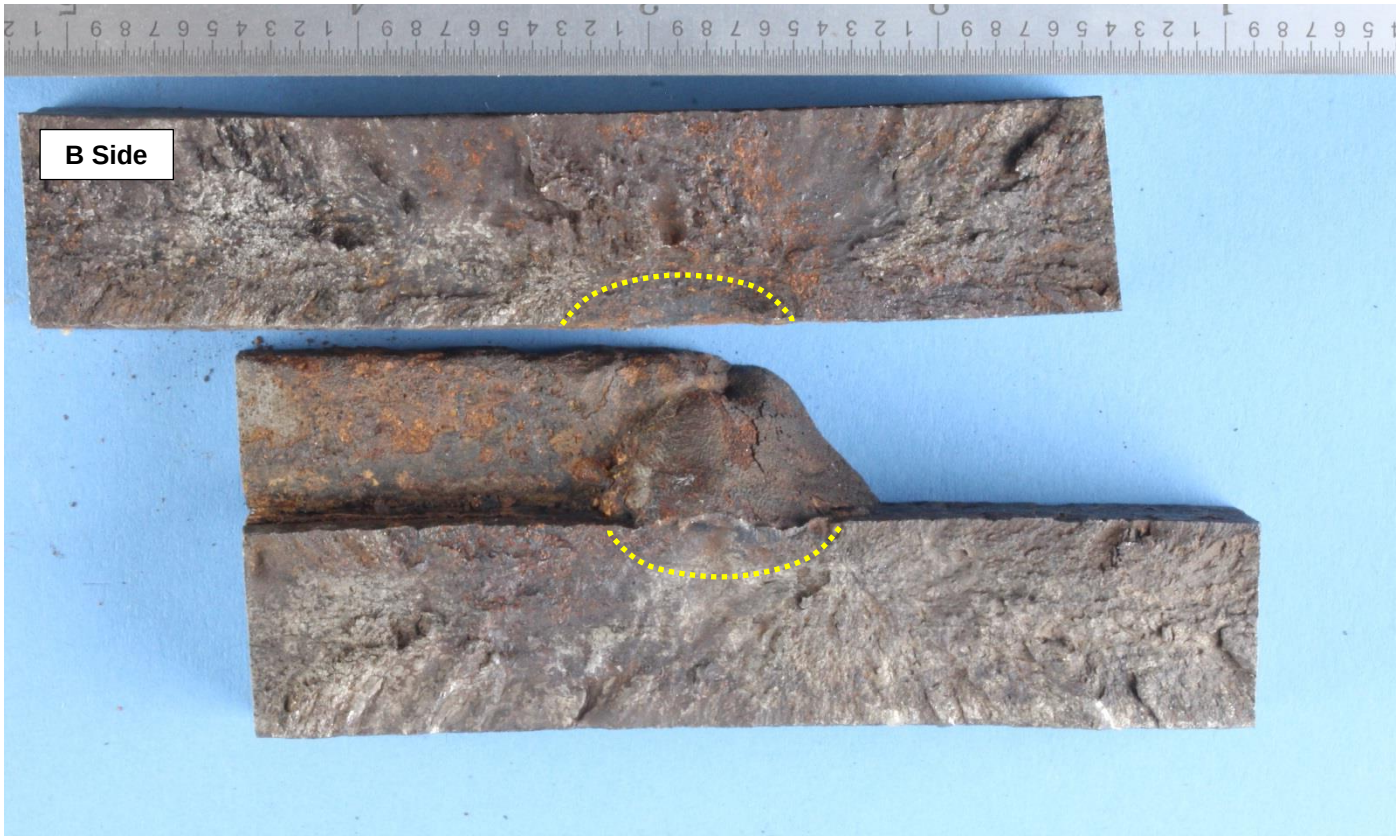

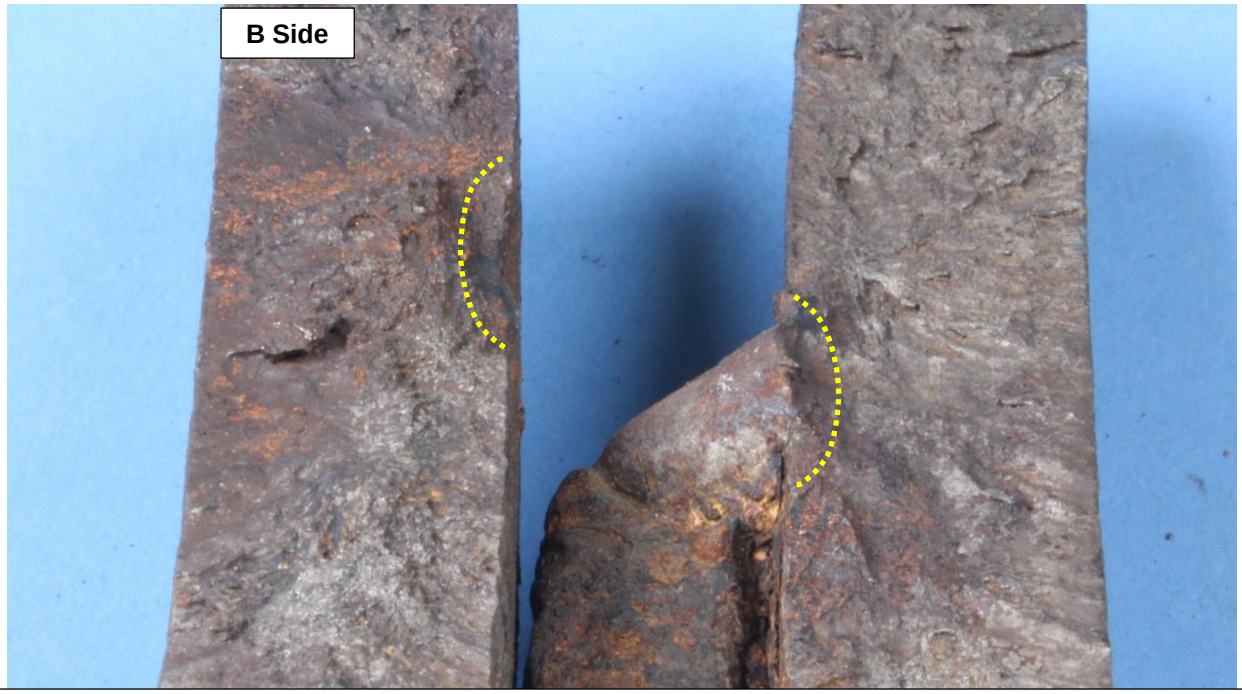

Figure 9. Two views of the mating fracture faces showing the initiation area at the toe of the repair weld with the dotted lines indicating the dark oxide region. Upper view is looking straight at the fracture surface while the lower view is at an oblique angle showing the angled orientation of the oxide region.

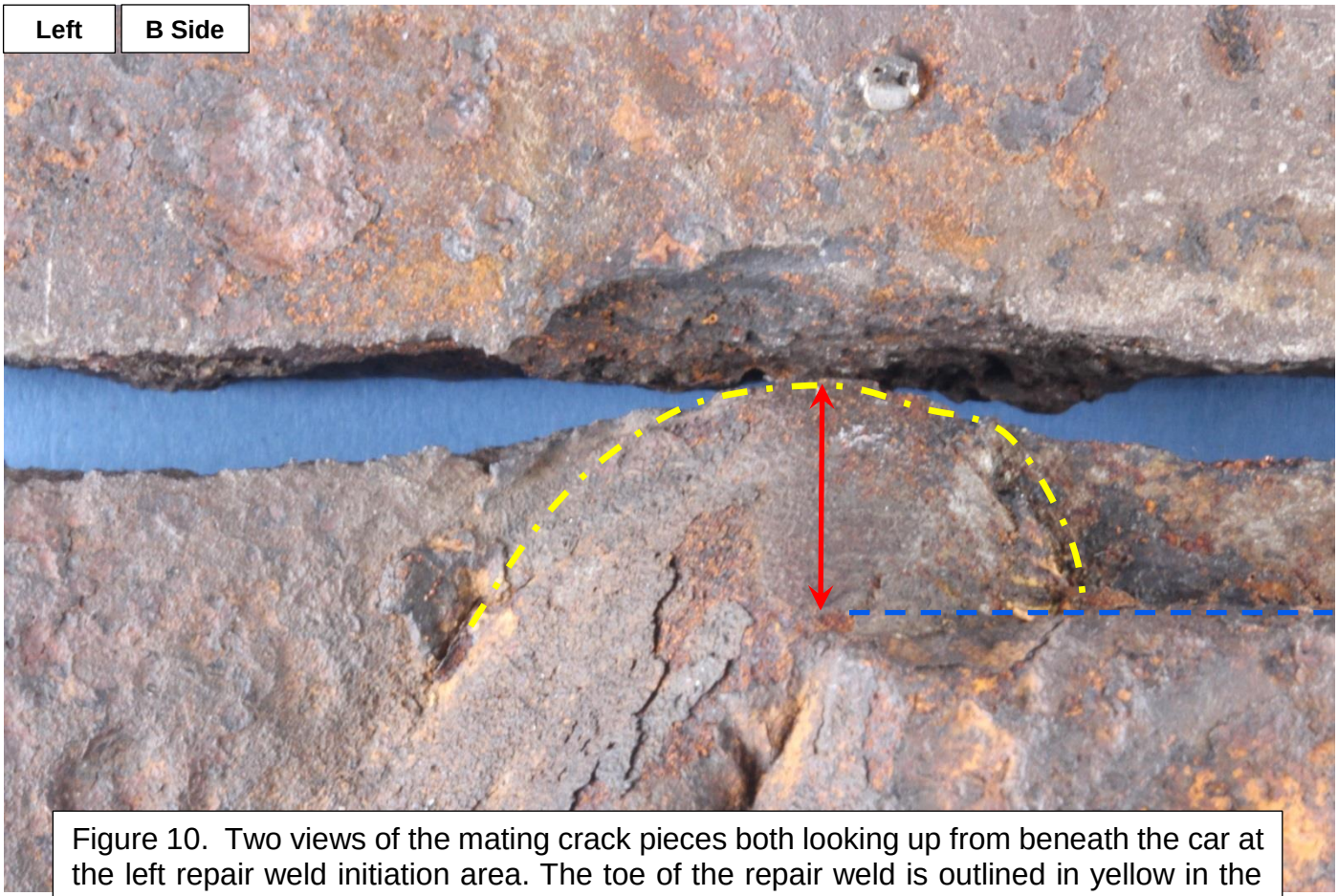

Figure 10. Two views of the mating crack pieces both looking up from beneath the car at the left repair weld initiation area. The toe of the repair weld is outlined in yellow in the lower view with the blue line indicating the end of the cradle pad. Green arrows in the upper view denote some of the corrosion pits in the outer surface of the tank.

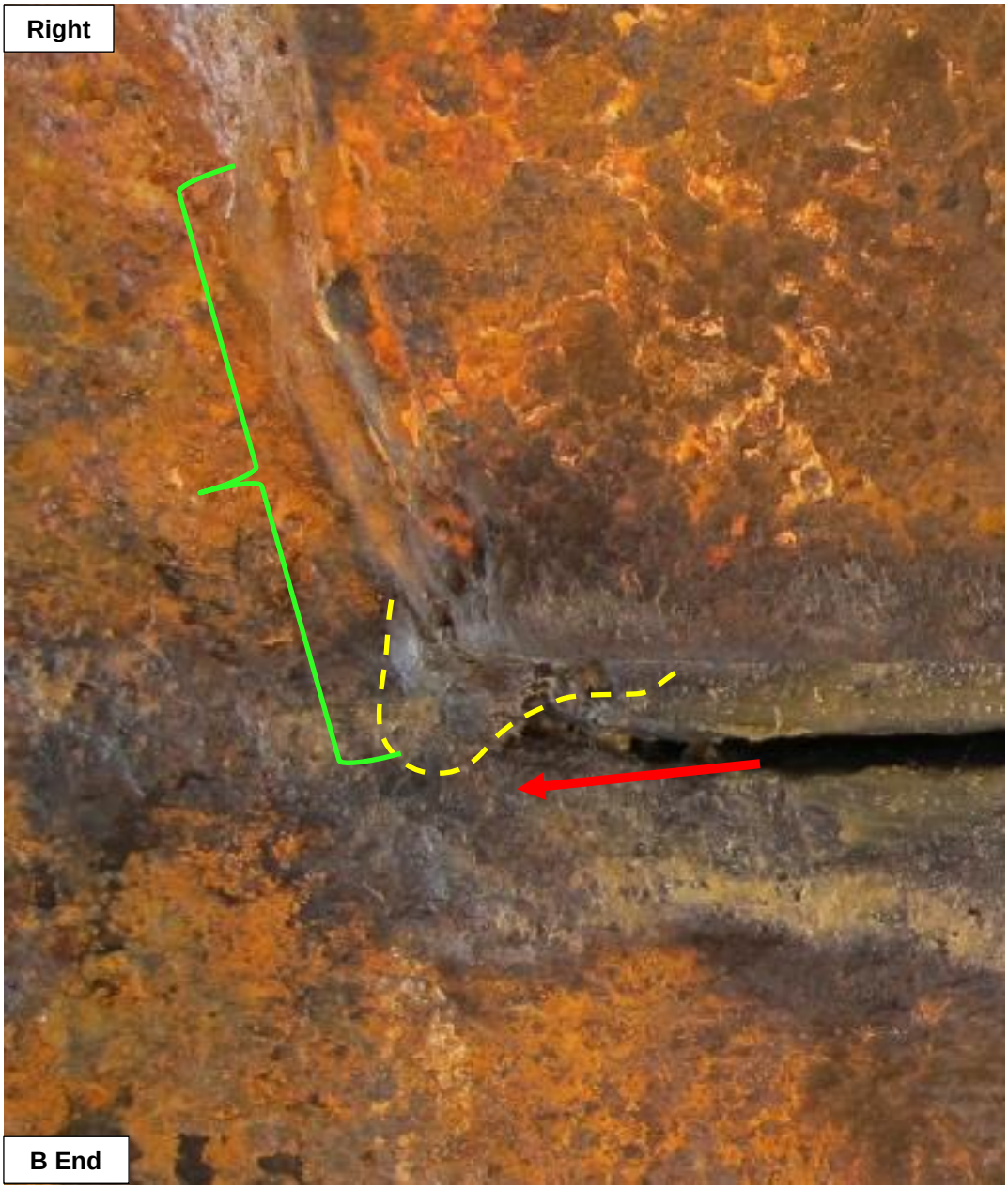

Figure 11. An intact view showing the relationship between the right end (red arrow) of the crack and the nearby right side repair weld (green bracket) with surfaces covered by preservative. The inboard toe of the weld is outlined in yellow.

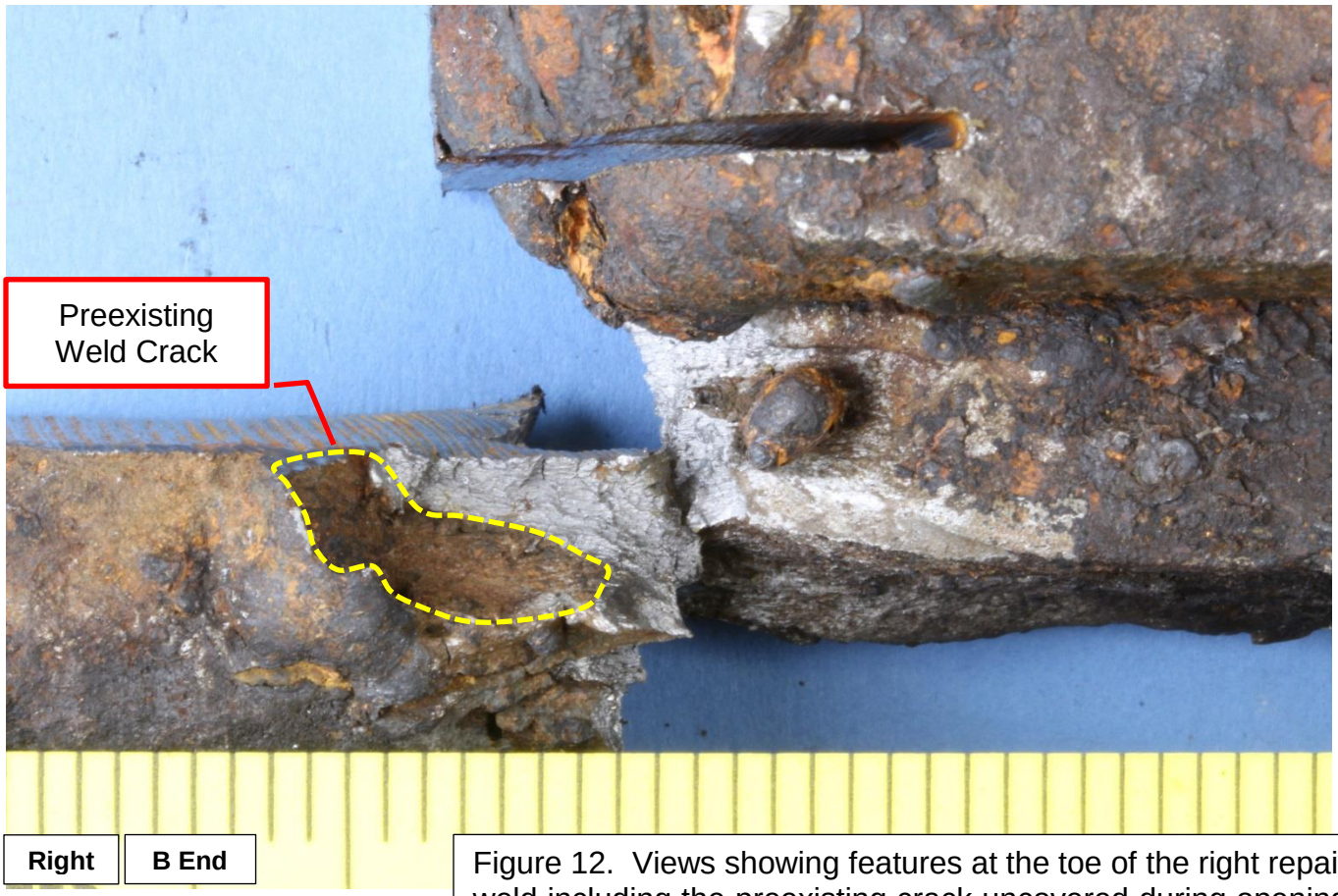

Figure 12. Views showing features at the toe of the right repair weld including the preexisting crack uncovered during opening of the large crack. A large surface connected pore, areas of lack of fusion and undercutting and melt balls are also denoted.

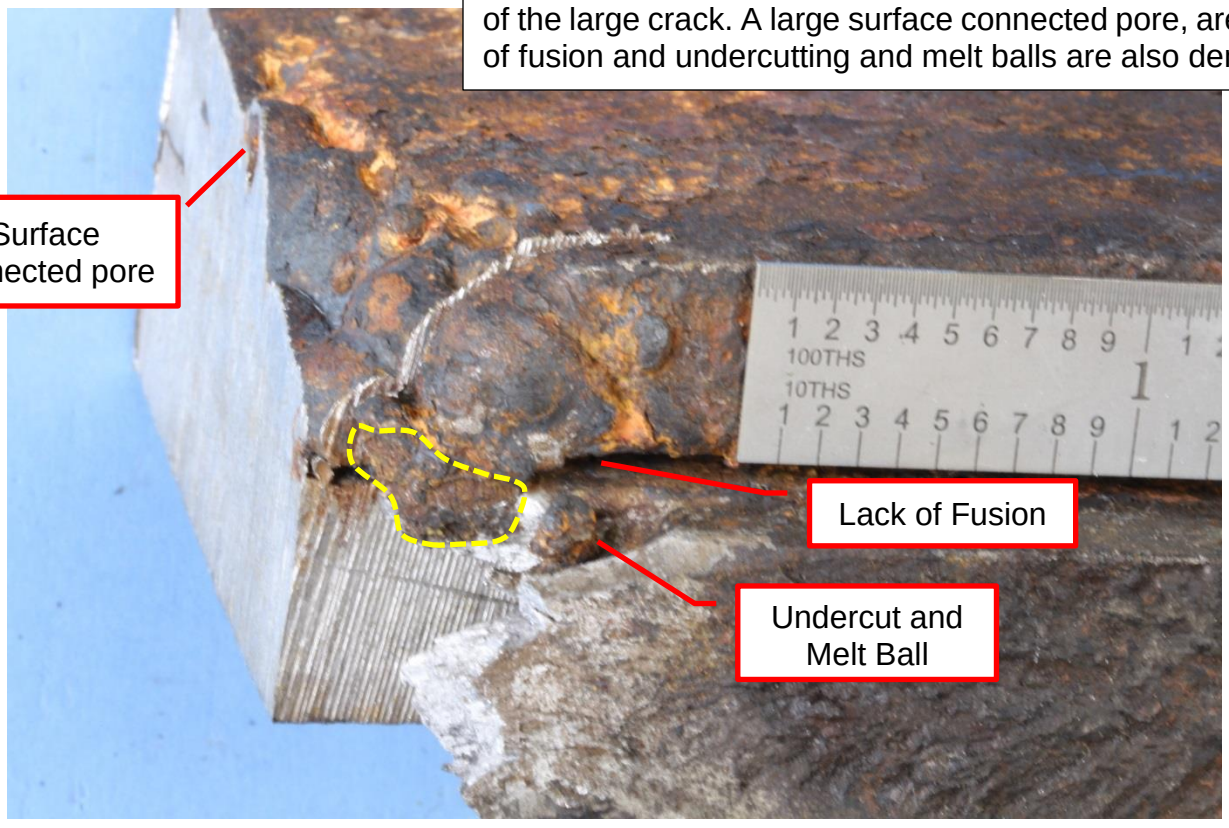

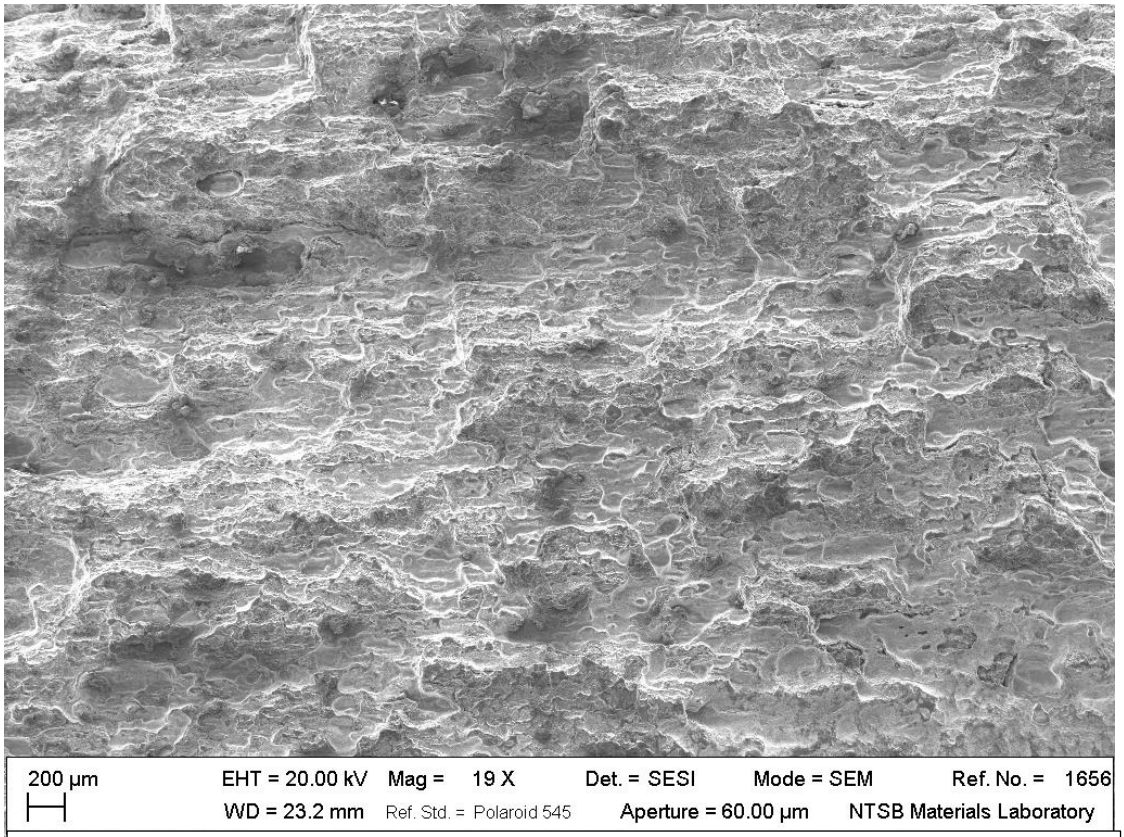

Figure 13. SEM views of the B side crack face in the initiation area showing woody fracture features above and a heavy oxide layer below.

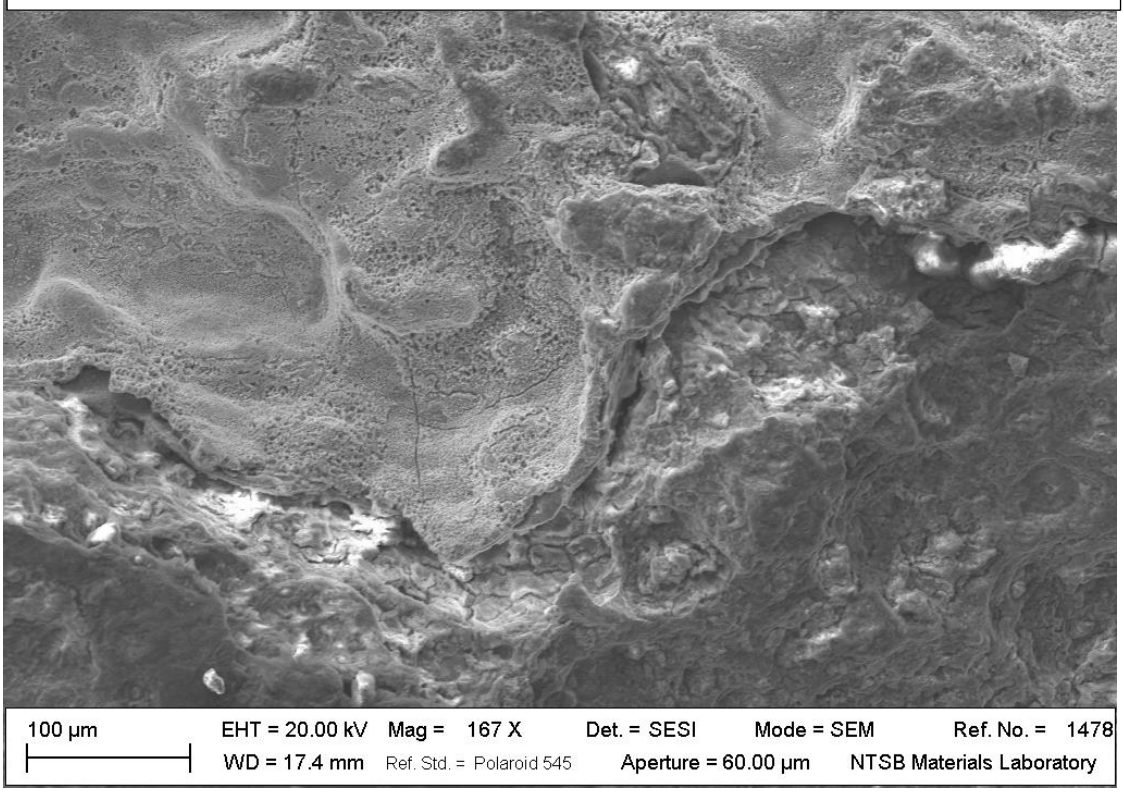

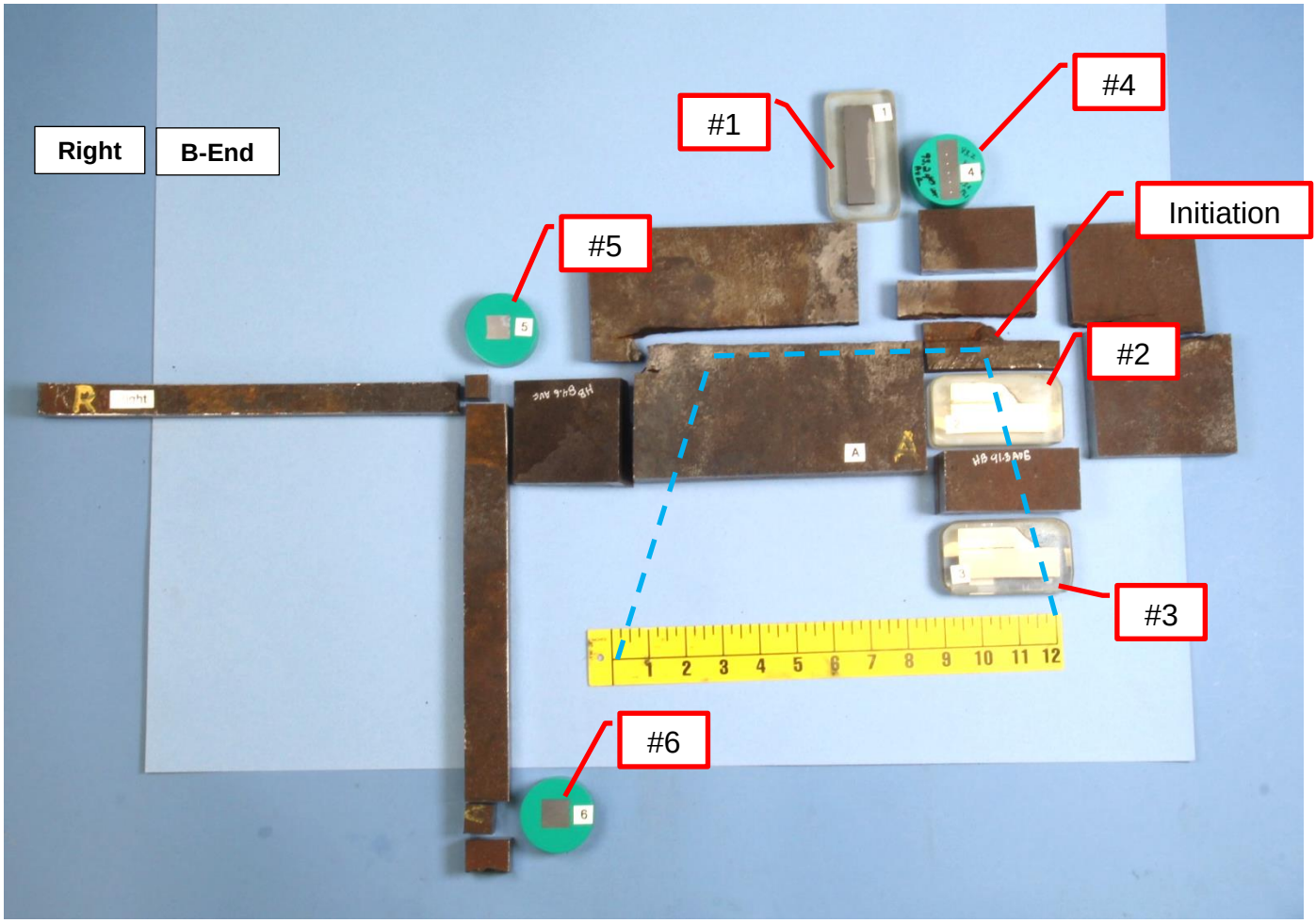

Figure 14. Layout of cut sections showing locations and relationships of the metallographic sections viewed from the interior surface. Approximate cradle pad location outlined in blue.

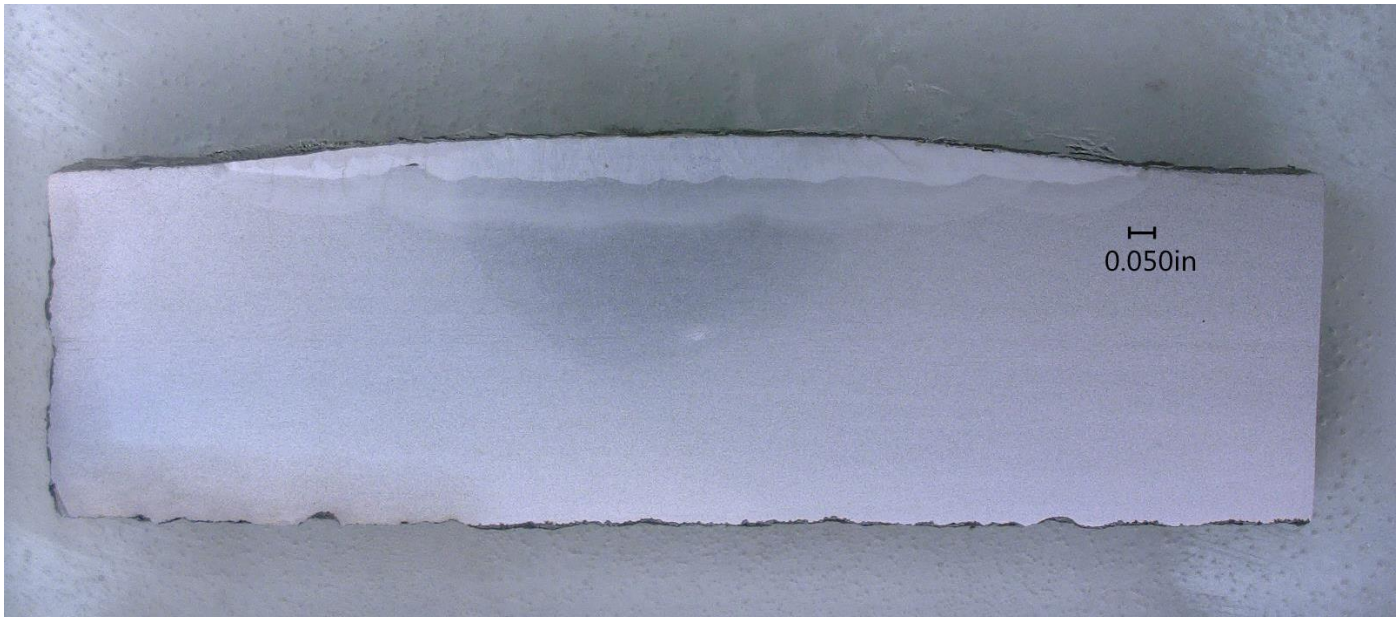

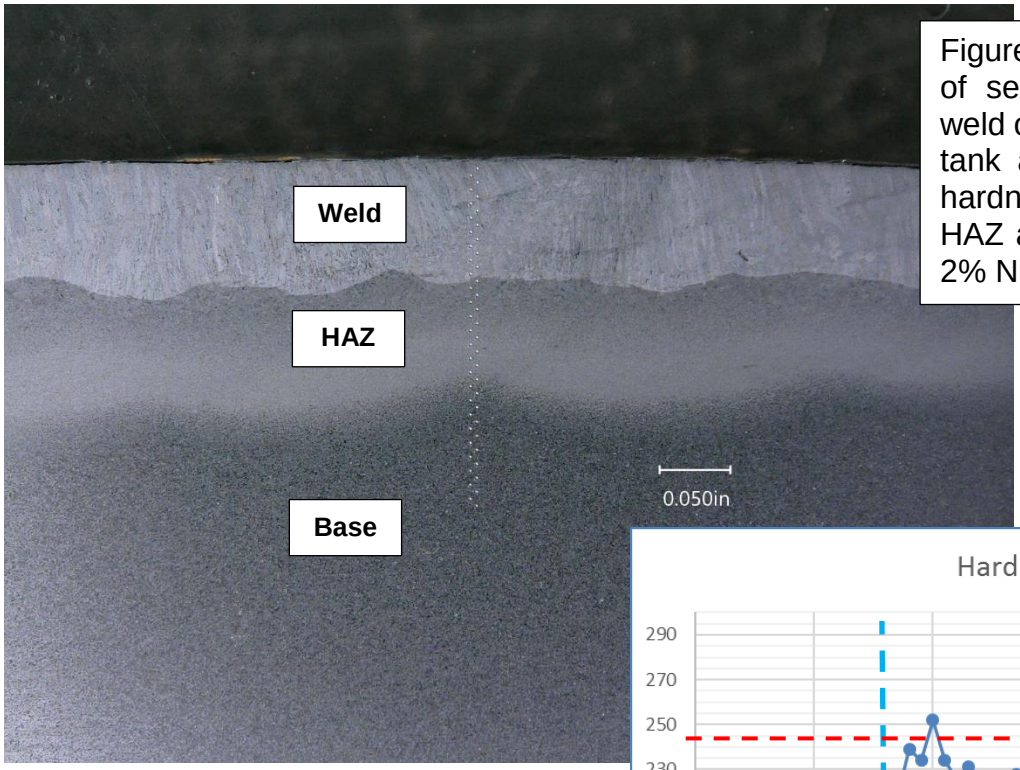

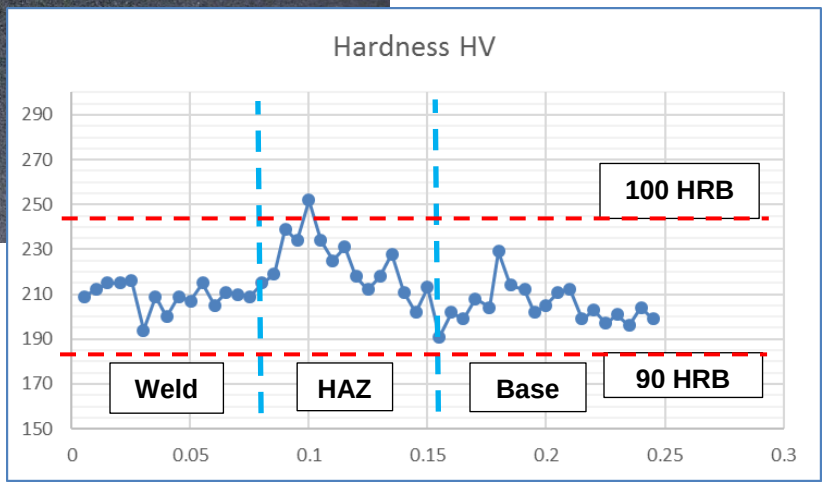

Figure 15. Metallographic views of section #1 through a repair weld on the interior surface of the tank at left and above. Vickers hardness, profile across weld, HAZ and into base metal below. 2% Nital Etch.

Figure 16. Metallographic views of section #2 through the repair weld on the left side of the A end cradle pad showing HAZ cracking with slag and lack of fusion between beads. Vickers hardness, profile across weld, HAZ and into base metal below in middle.

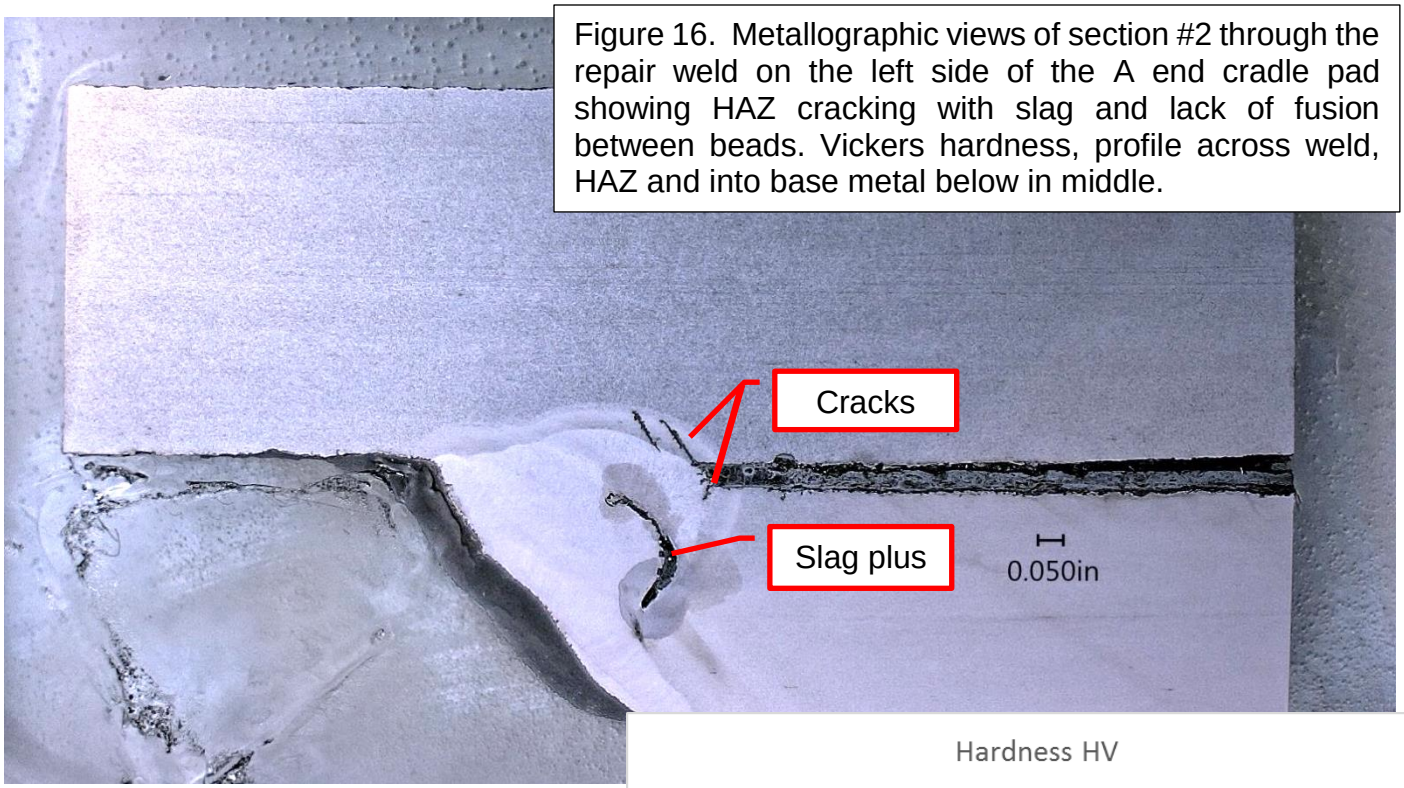

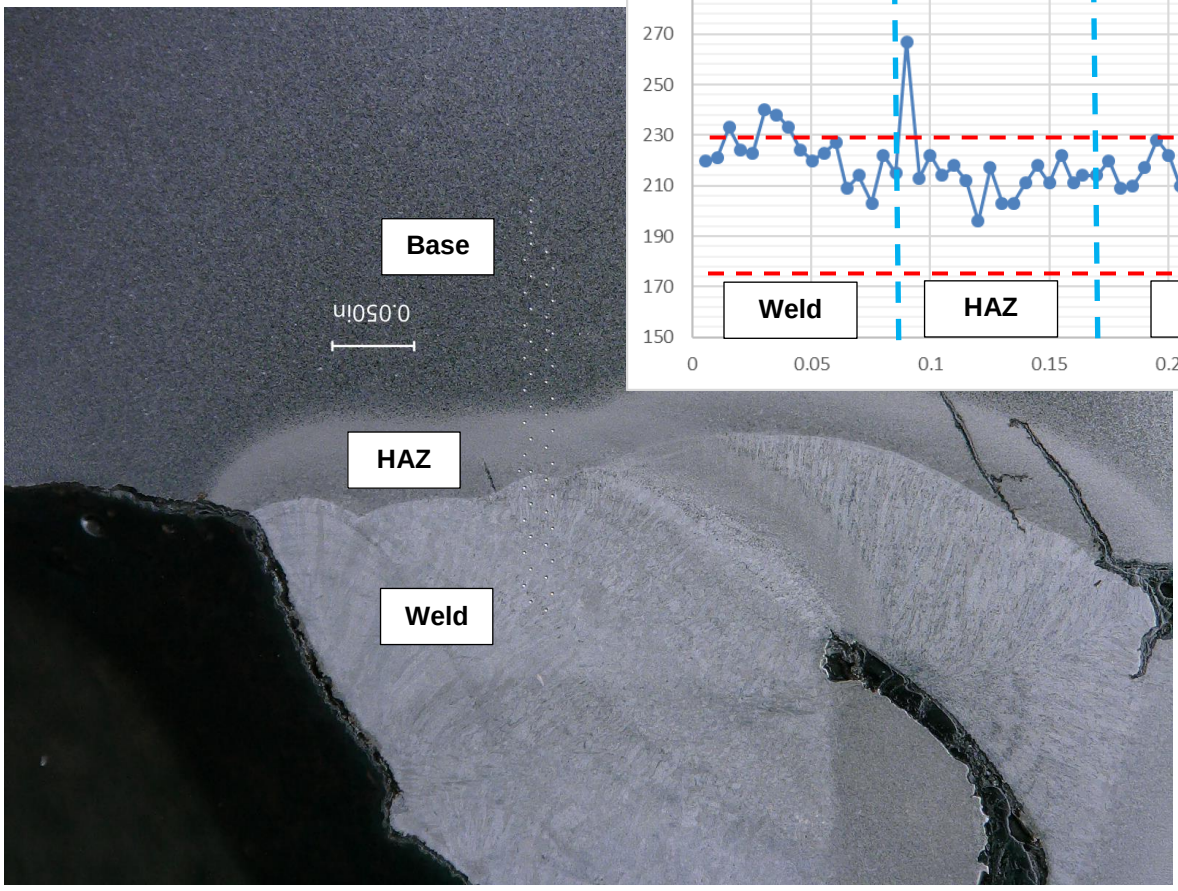

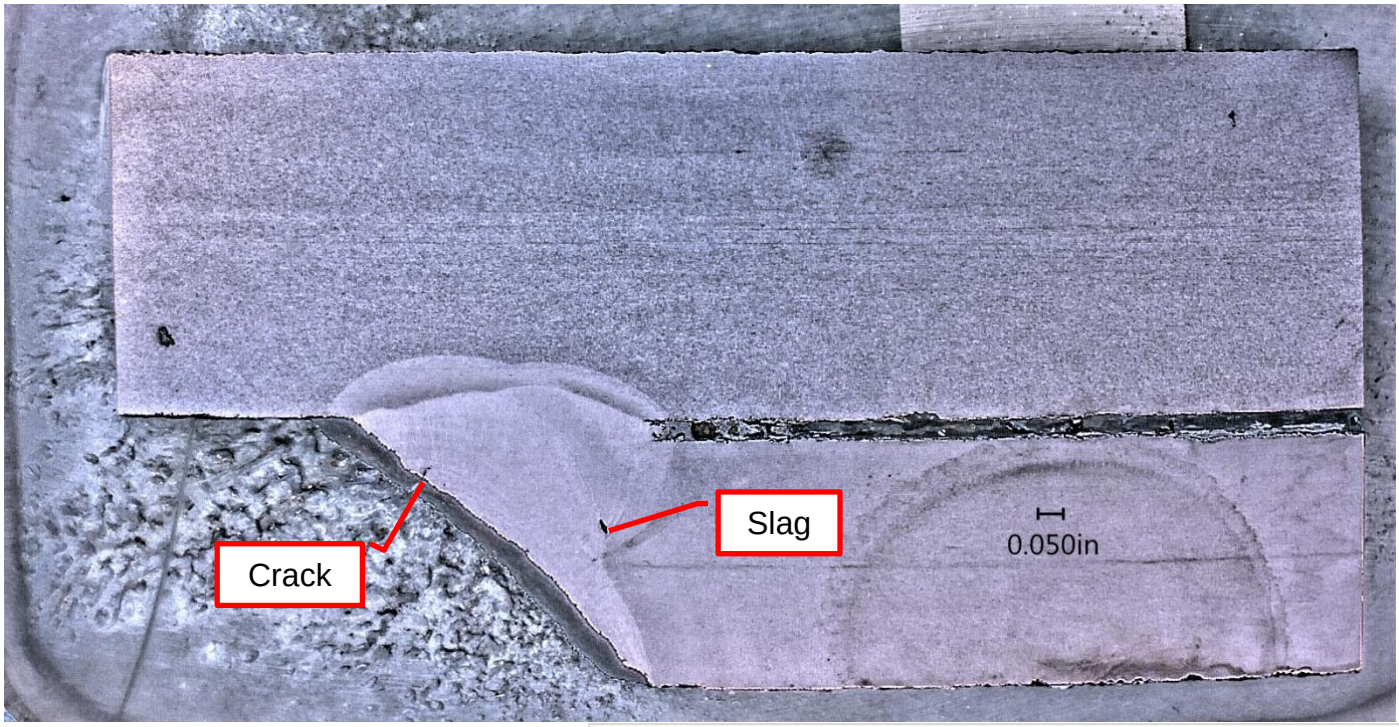

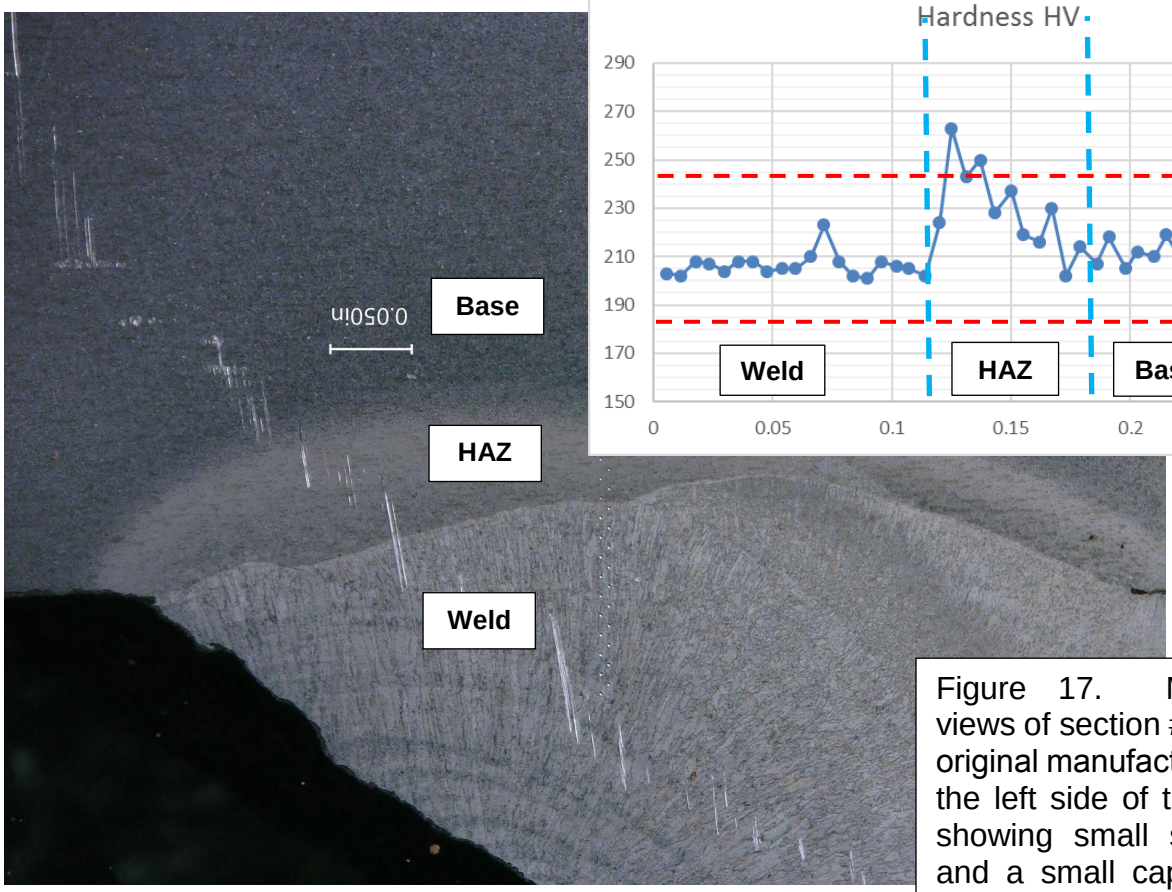

Figure 17. Metallographic views of section #3 through the original manufacturer's weld on the left side of the cradle pad showing small slag inclusion and a small cap bead crack. Vickers hardness profile across weld, HAZ and into base metal in middle. 2%Nital

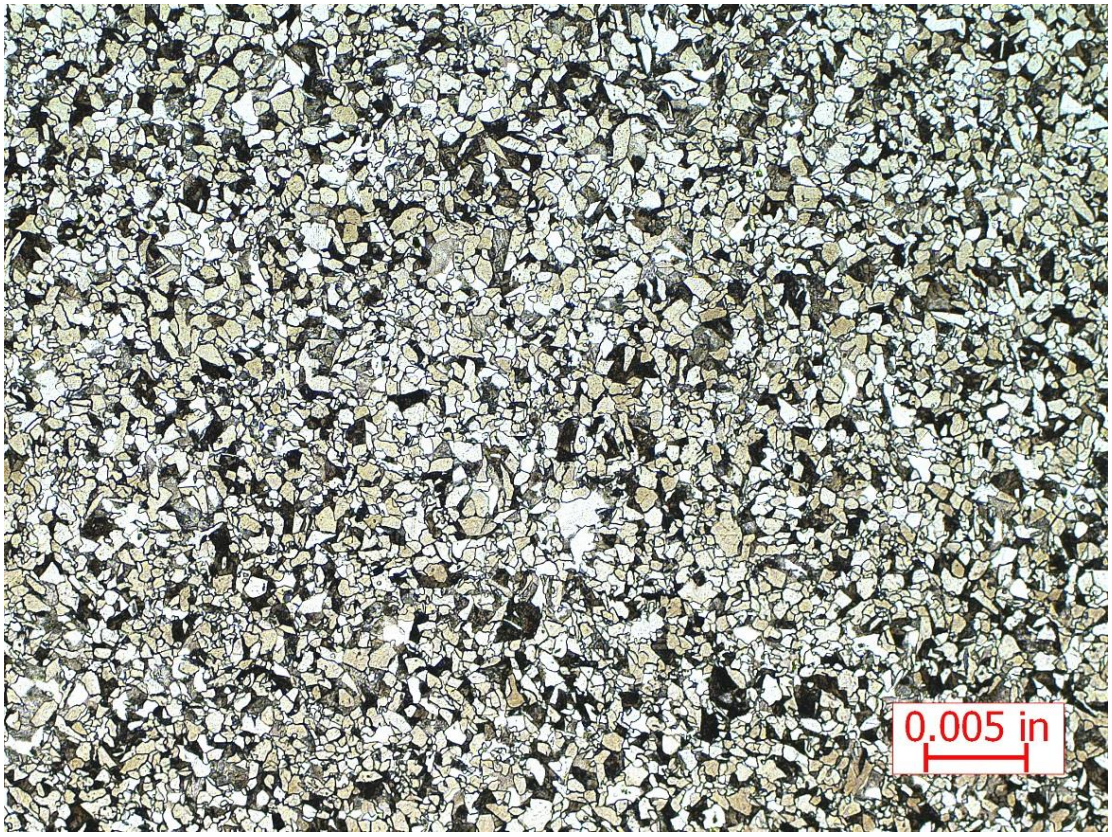

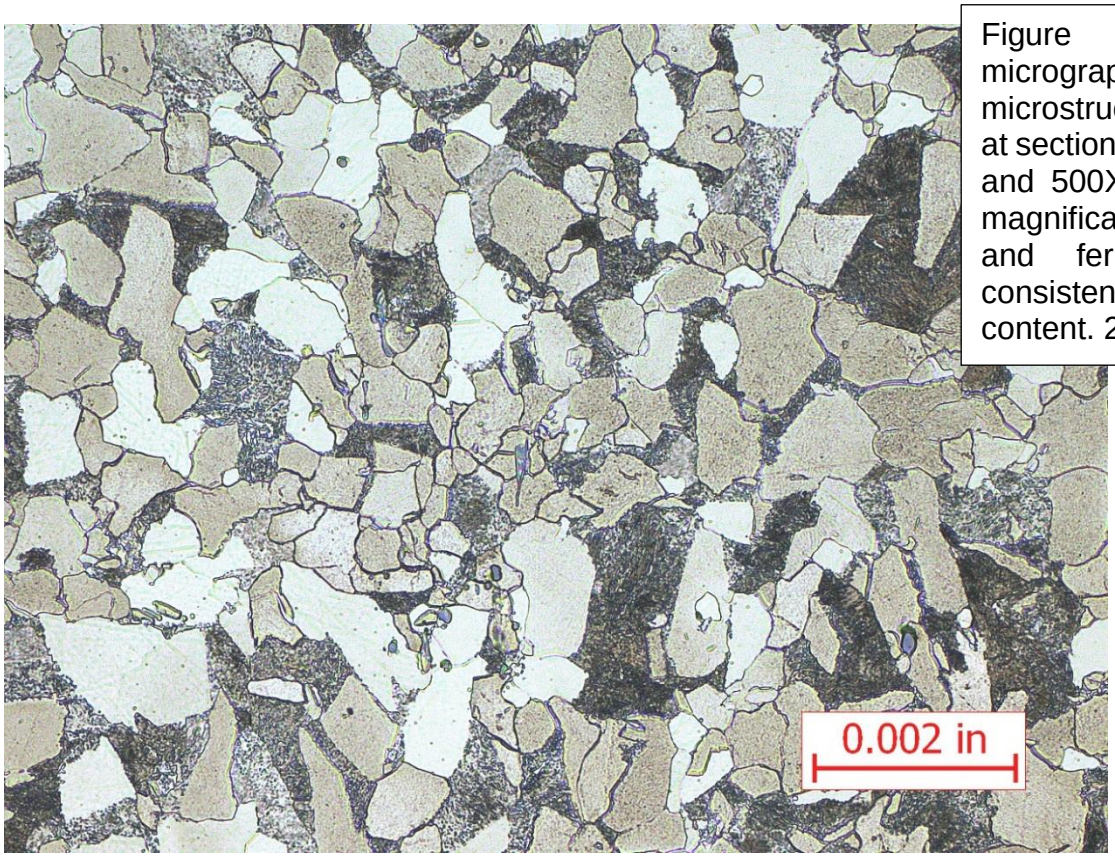

Figure 18. Optical micrographs of the microstructure of the tank at section #4, 100X above and 500X below original magnifications. Pearlite and ferrite in ratios consistent with the carbon content. 2% Nital.

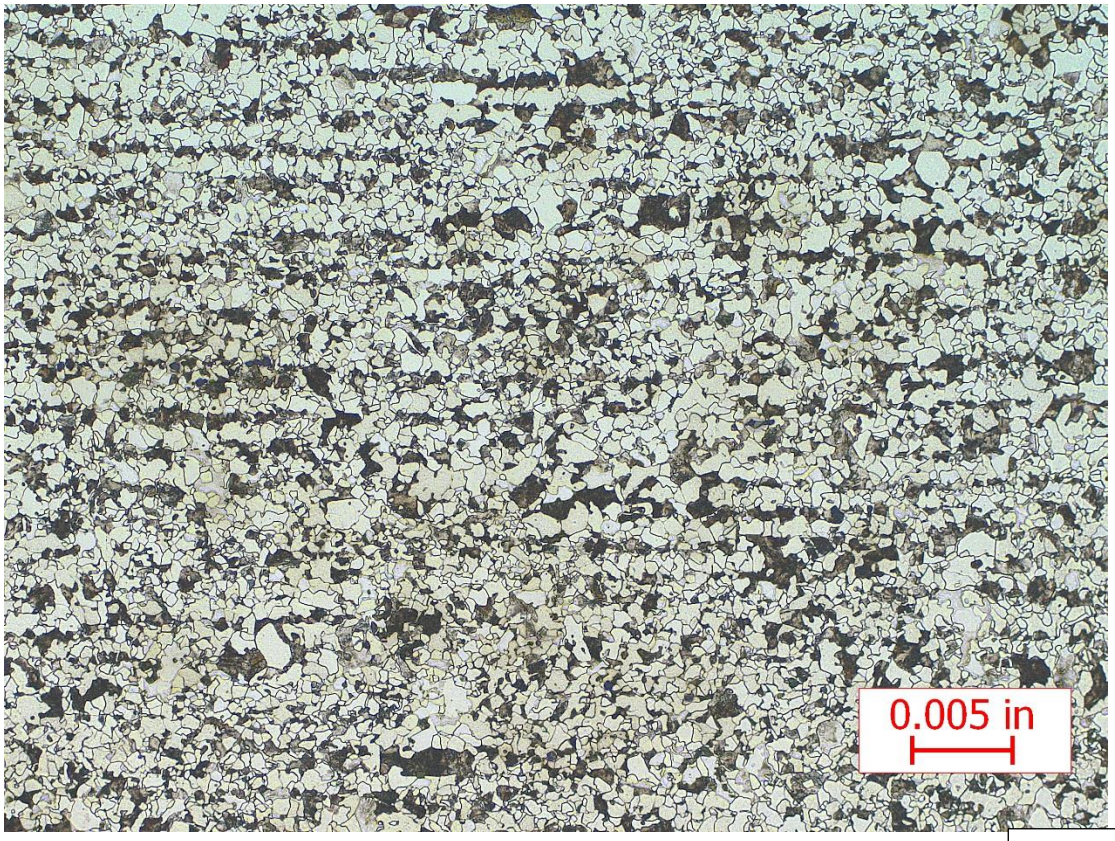

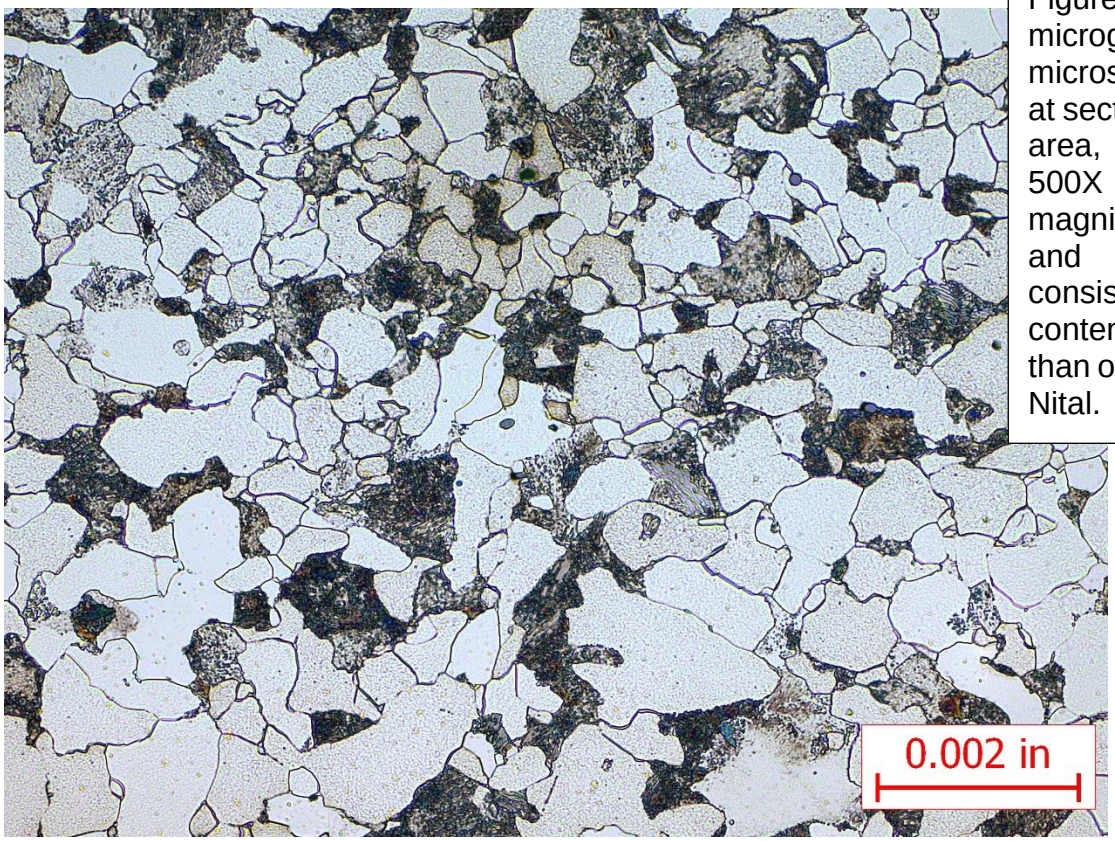

Figure 19. Optical micrographs of the microstructure of the tank at section #5 in the scaled area, 100X above and 500X below original magnifications. Pearlite and ferrite in ratios consistent with the carbon content. More banding than other specimens. 2% Nital.

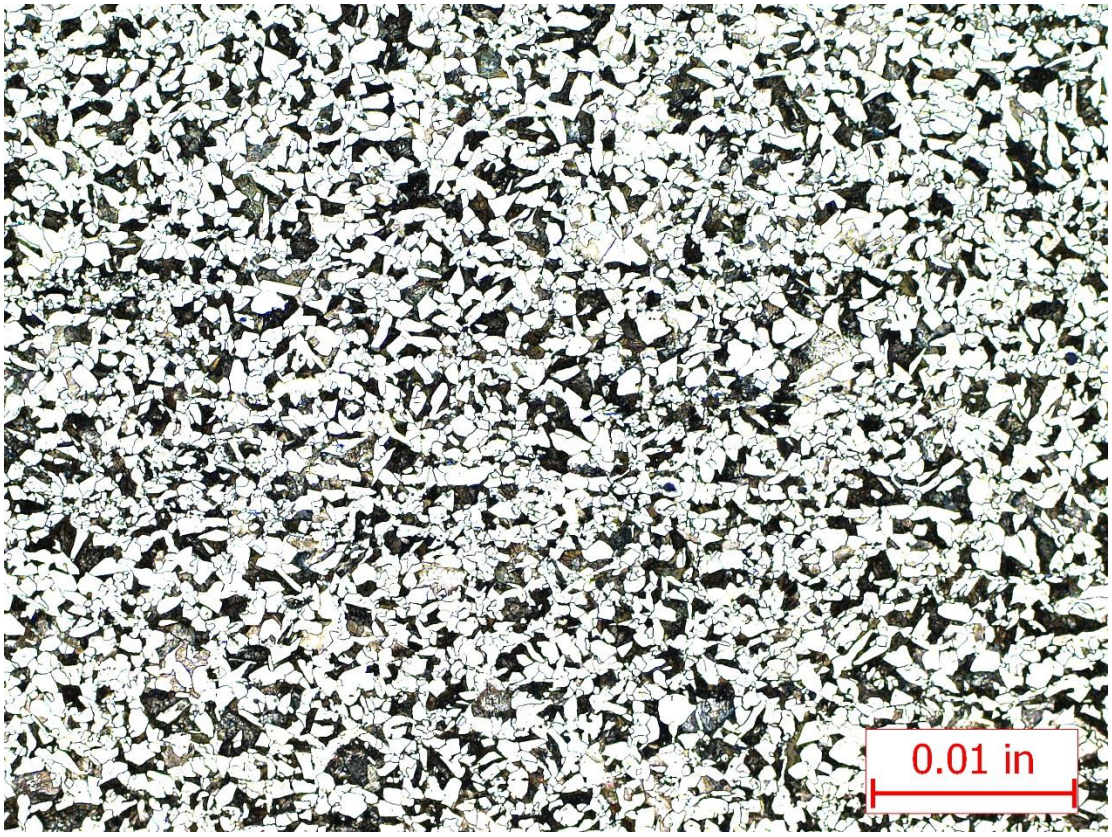

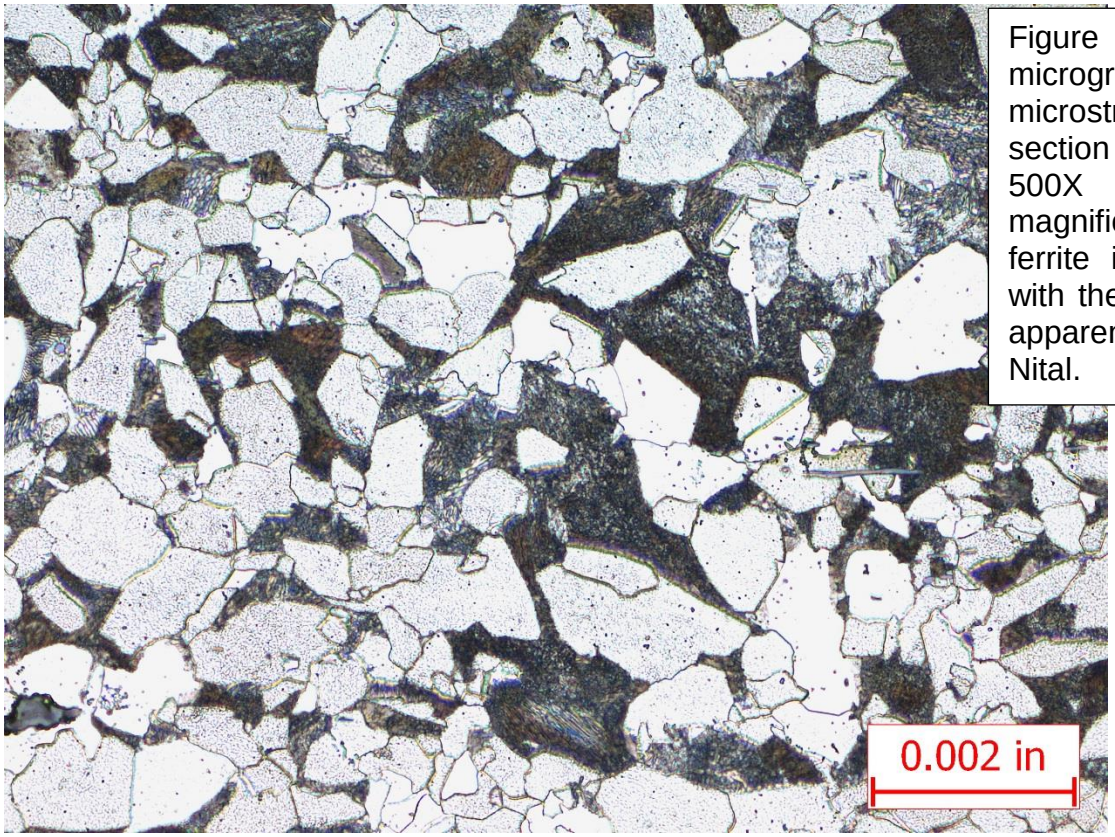

Figure 20. Optical micrographs of the microstructure of the tank at section #6, 100X above and 500X below original magnifications. Pearlite and ferrite in ratios consistent with the carbon content no apparent banding . 2% Nital.

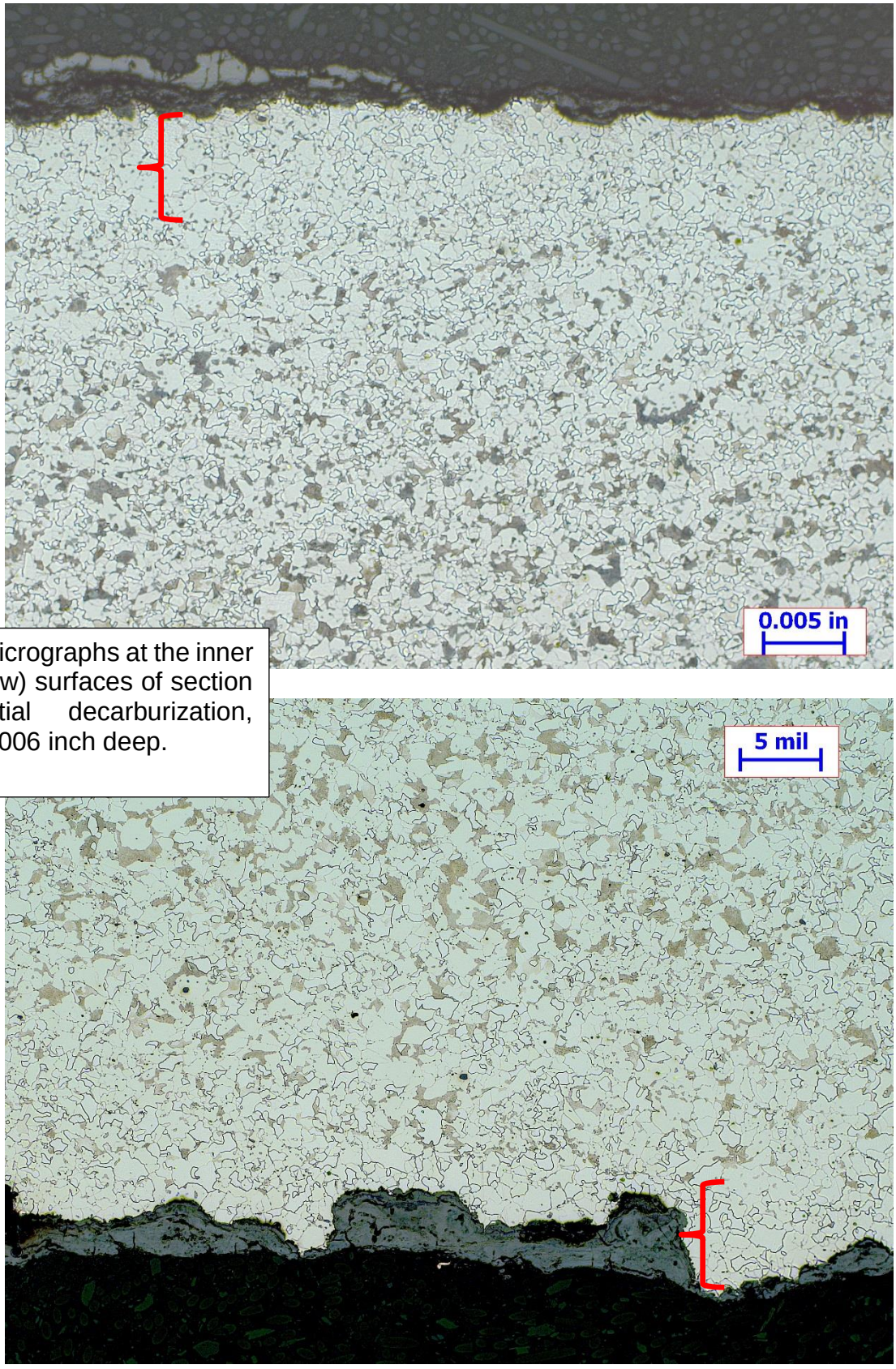

Figure 21. Optical micrographs at the inner (top) and outer (below) surfaces of section #5 showing partial decarburization, brackets, to about 0.006 inch deep. 2% Nital.

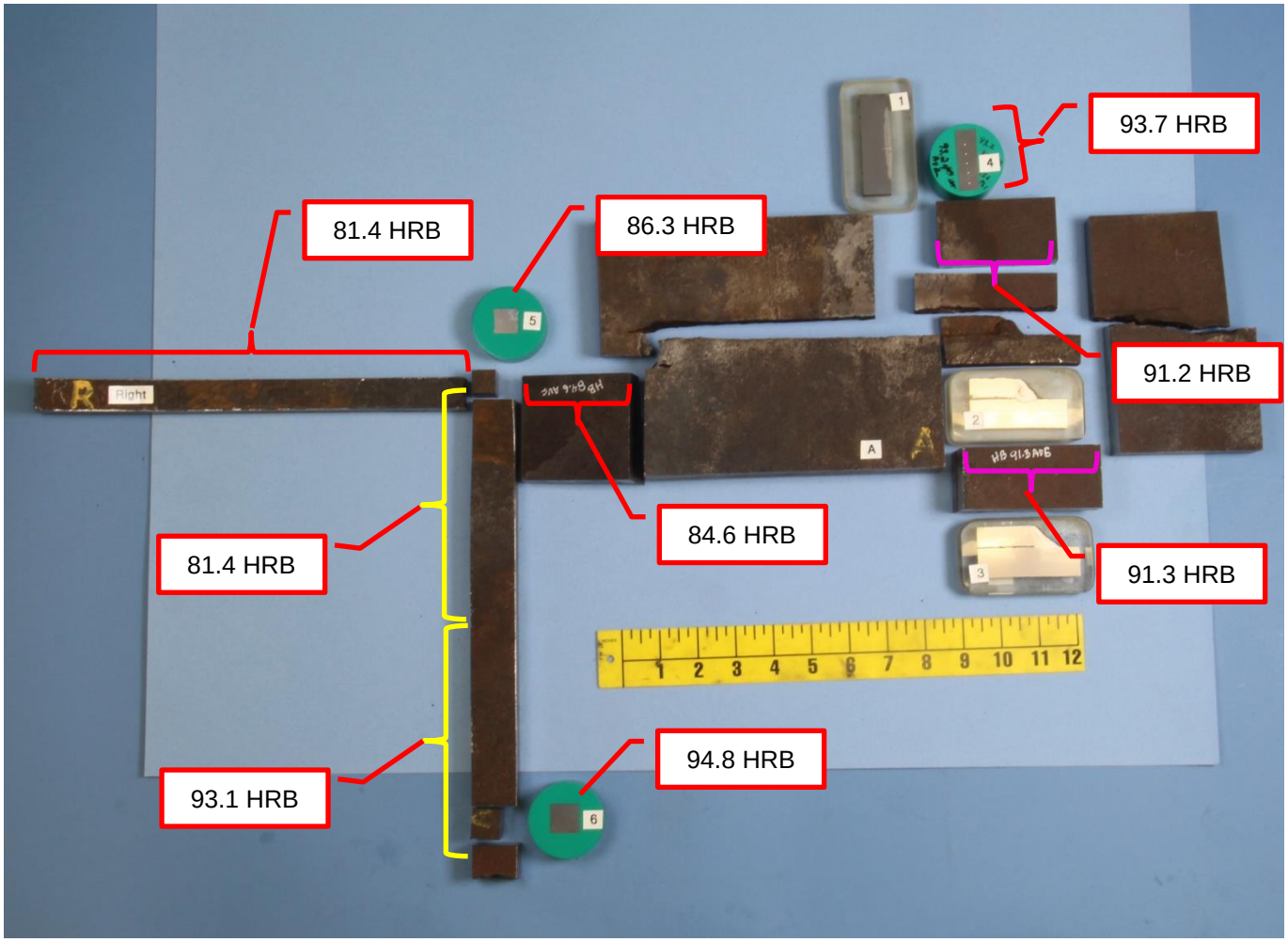

Figure 22. Average hardness measurements at different locations shown pictographically. Displayed values are averaged for each location. Thickness measurements were made at yellow and purple bracketed areas.

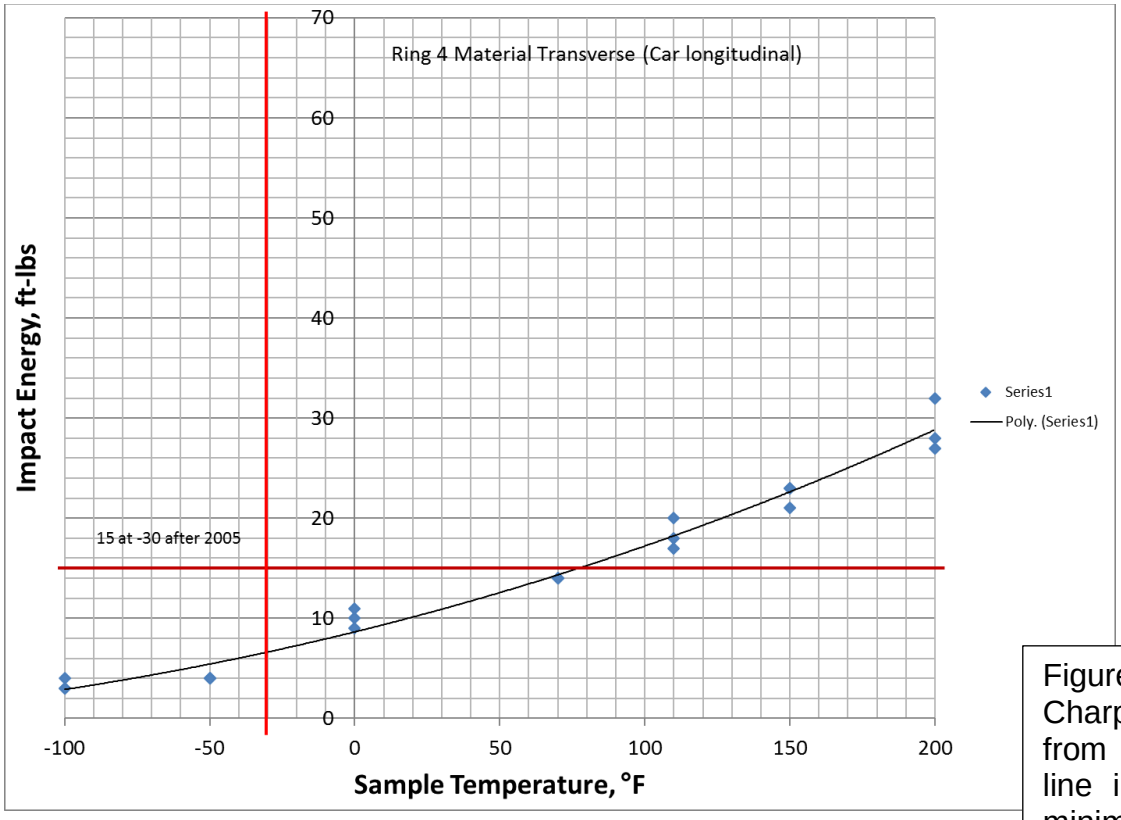

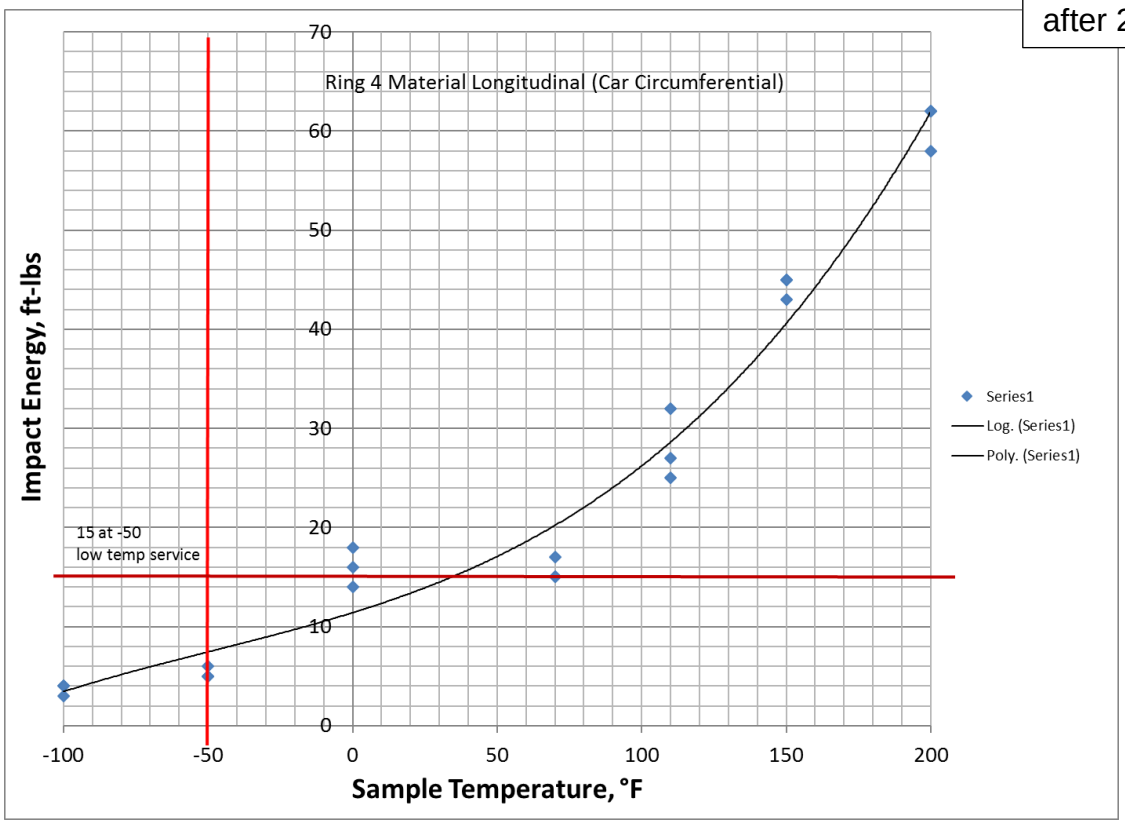

Figure 23. Graphs of Charpy impact results from ring 4 material. Red line intersections denote minimum requirements after 2005.

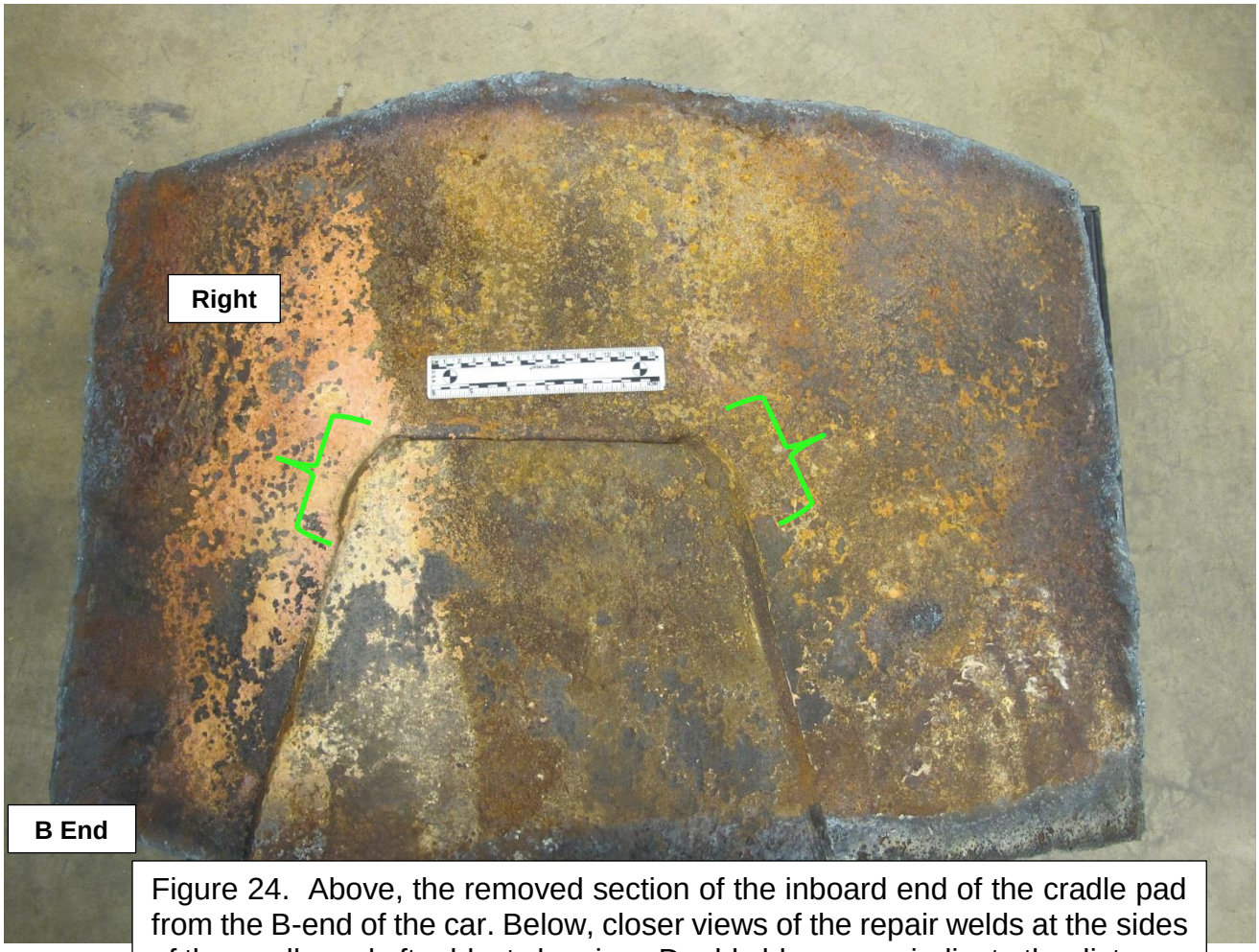

Figure 24. Above, the removed section of the inboard end of the cradle pad from the B-end of the car. Below, closer views of the repair welds at the sides of the cradle pad after blast cleaning. Double blue arrow indicate the distance between the welds.

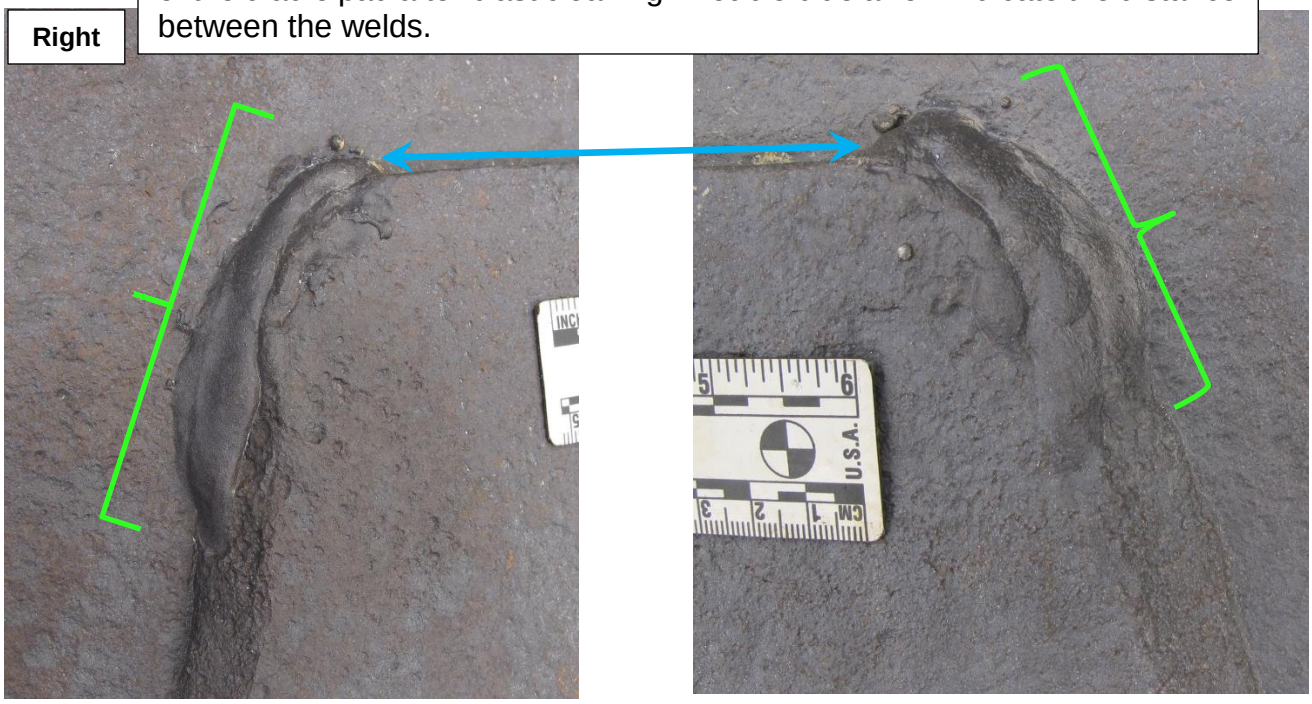

Figure 25. Two views of the inboard toe of the left repair weld on the B-end showing magnetic particle NDT indications (red brackets). Dry powder at top and fluorescent wet particle at right. Dashed lines indicate approximate location of metallographic section B15 through the indication.

Figure 26. View of the cut up B end cradle pad showing the locations of the metallographic sections.

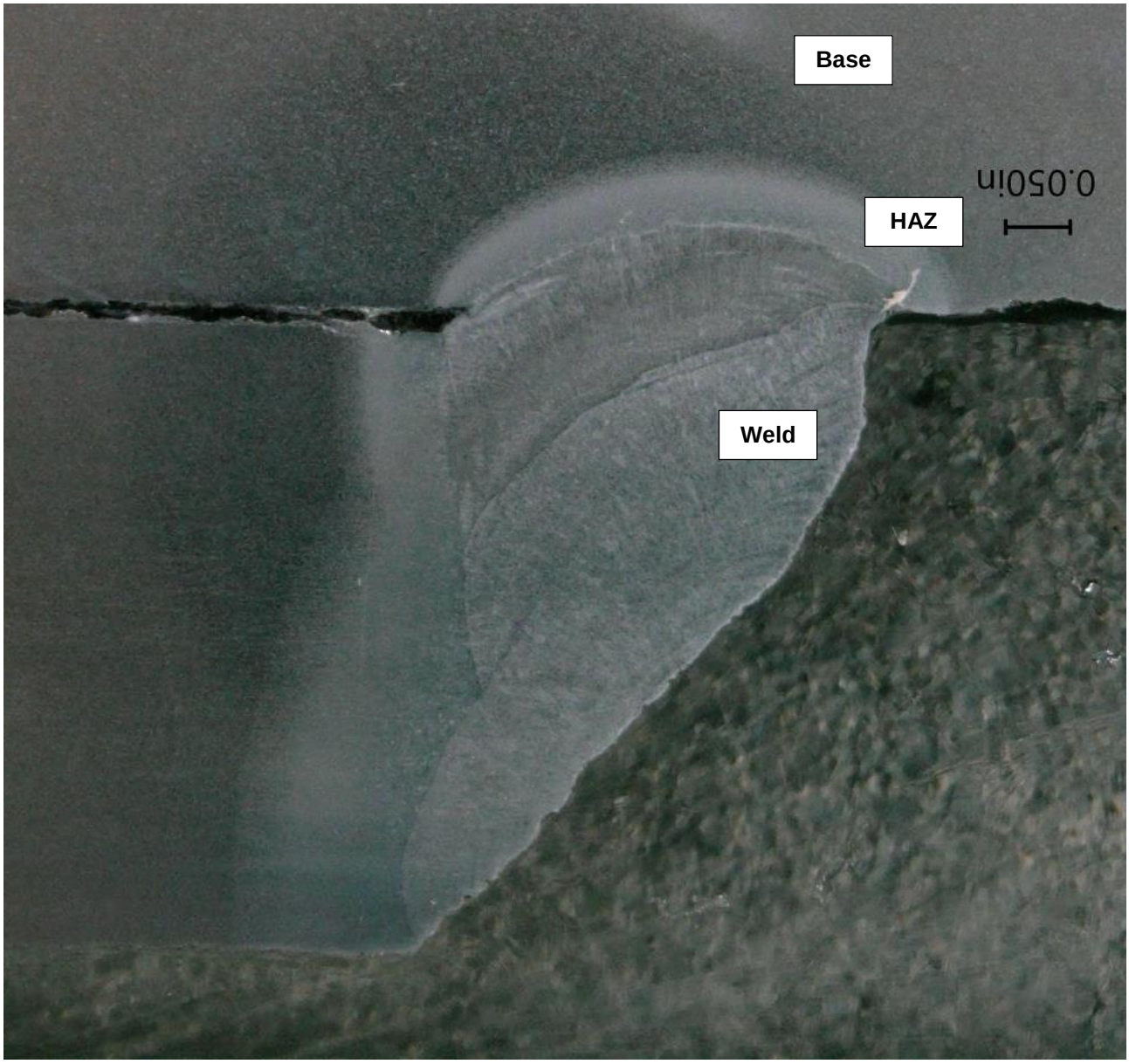

Figure 27. Optical micrographs of the microstructure of the B end right side original manufacturer weld. Sample B10, 2% Nital etch.

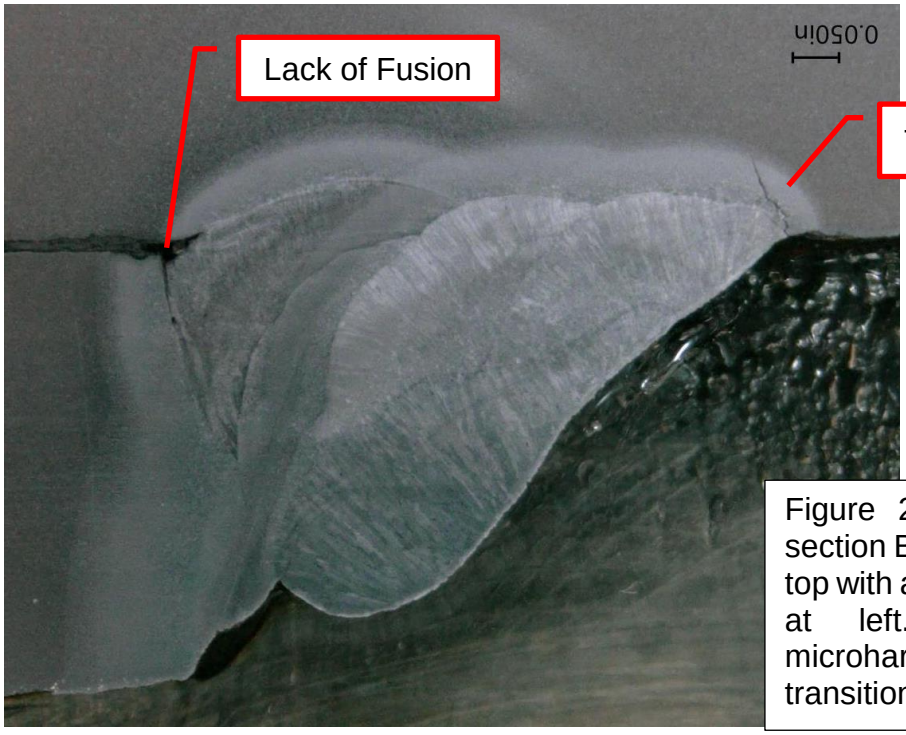

Figure 28. Optical micrographs of section B11 showing the overall weld at top with a close-up view of the toe crack at left. Graph shows Vickers microhardness traverse with weld zone transitions indicated. 2% Nital etch.

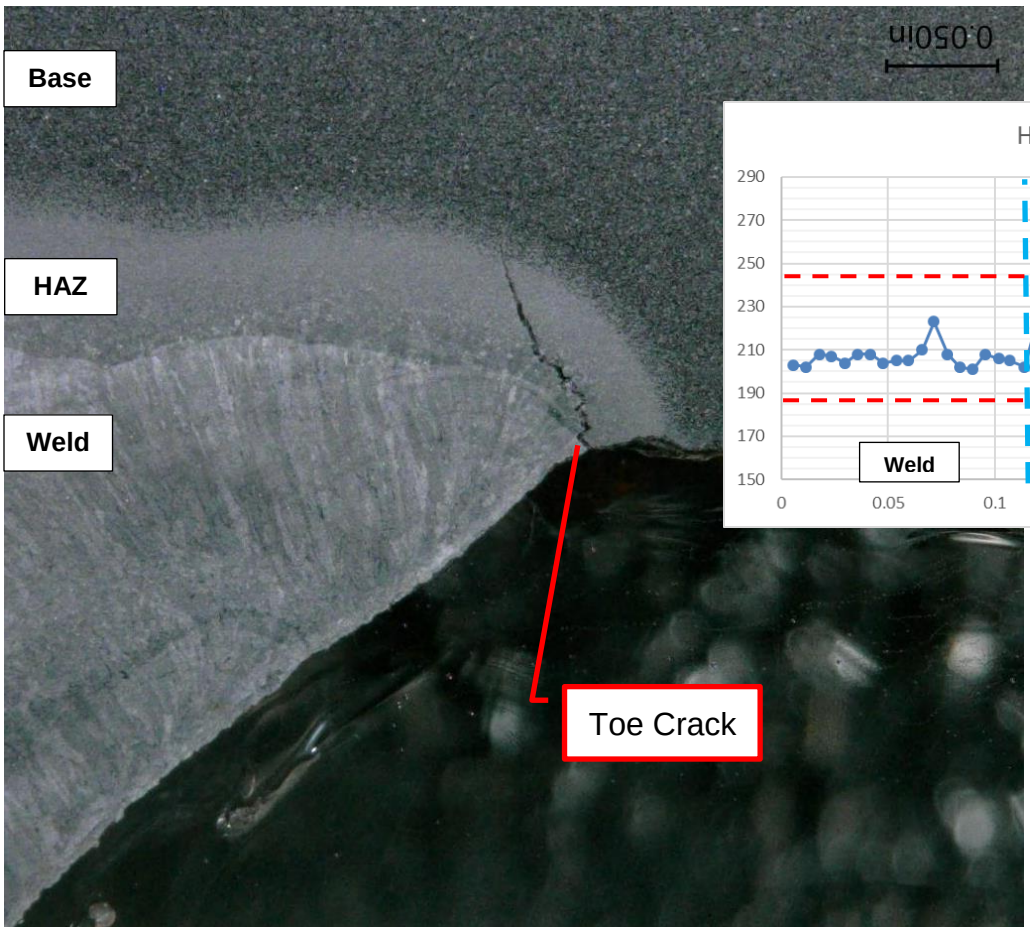

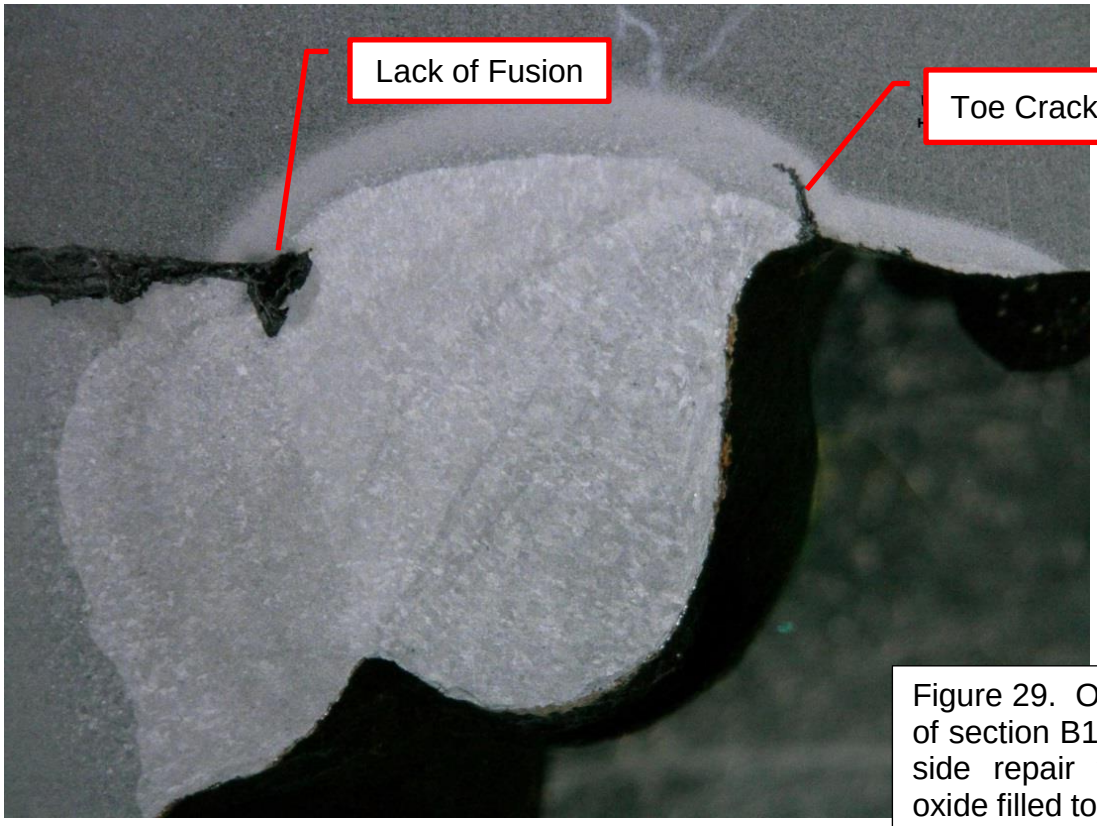

Figure 29. Optical micrographs of section B12 through the right side repair weld showing an oxide filled toe crack and lack of fusion at the root. 2% Nital Etch.

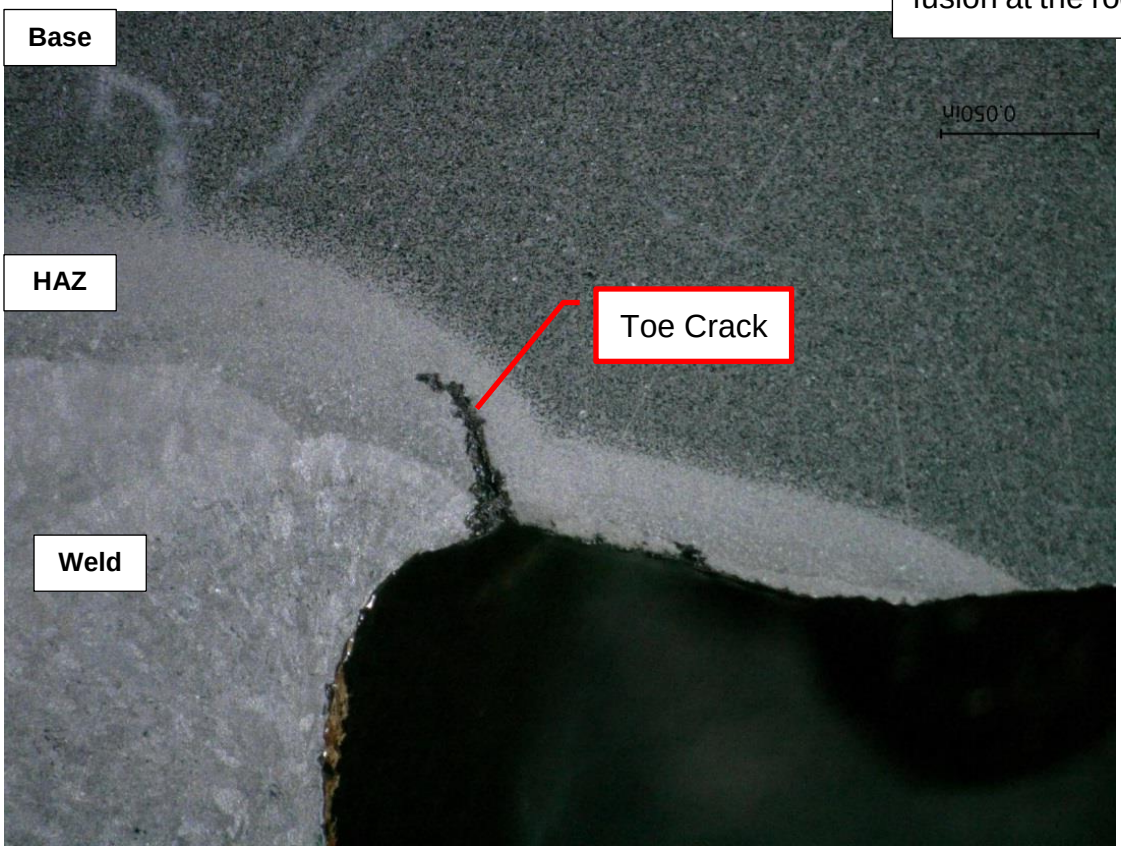

B13

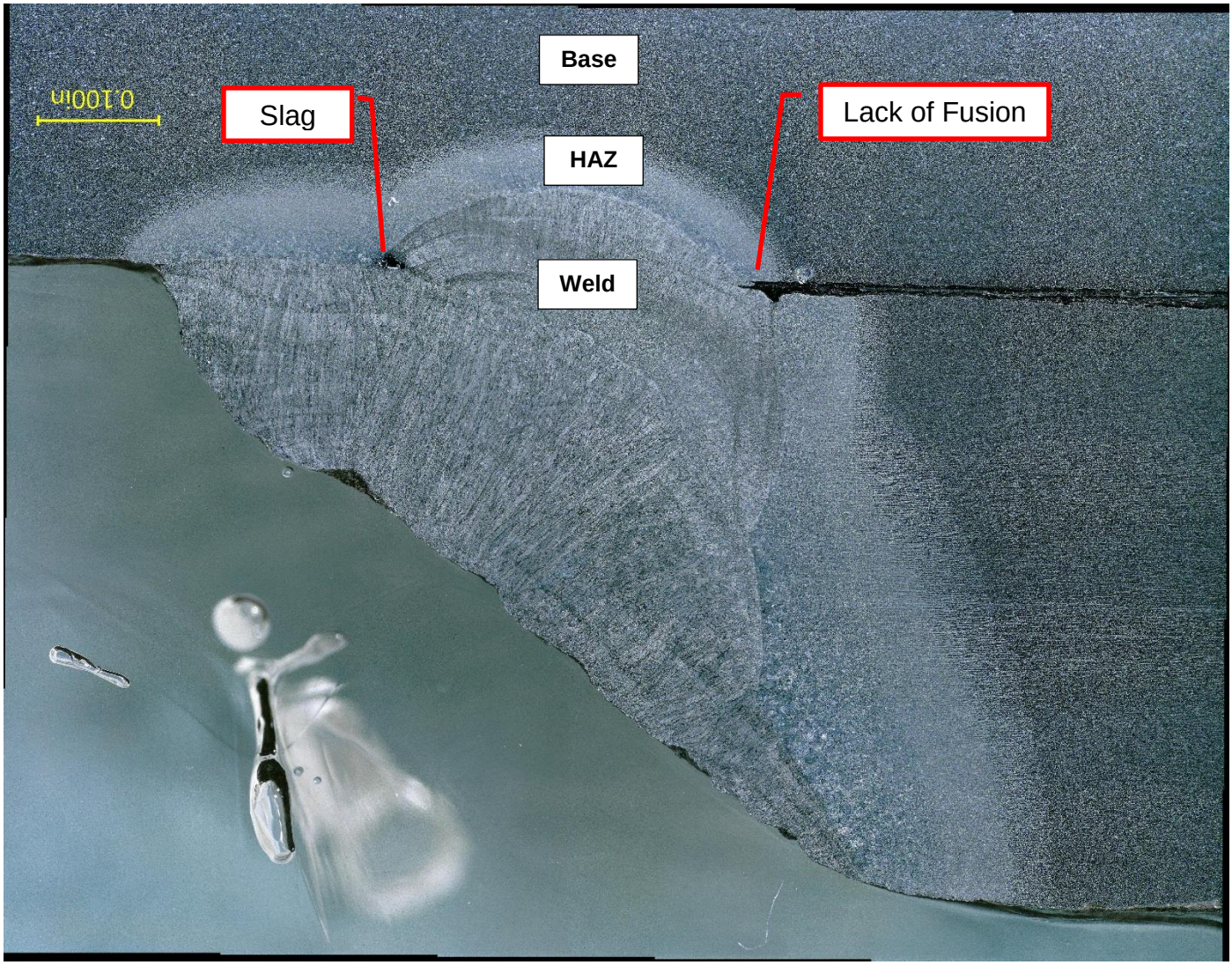

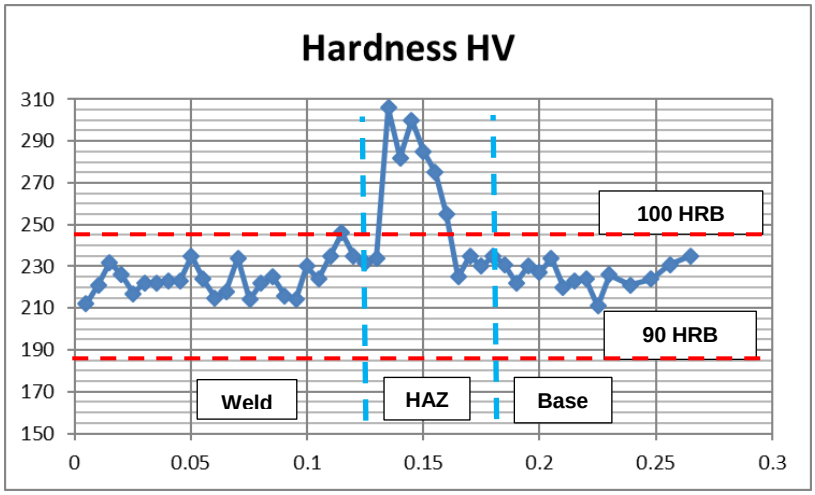

Figure 30. Optical micrograph of section B13 through the left side original weld, above, with slag and lack of fusion noted. 2% Nital etch.
Graph of Vickers hardness traverse at left.

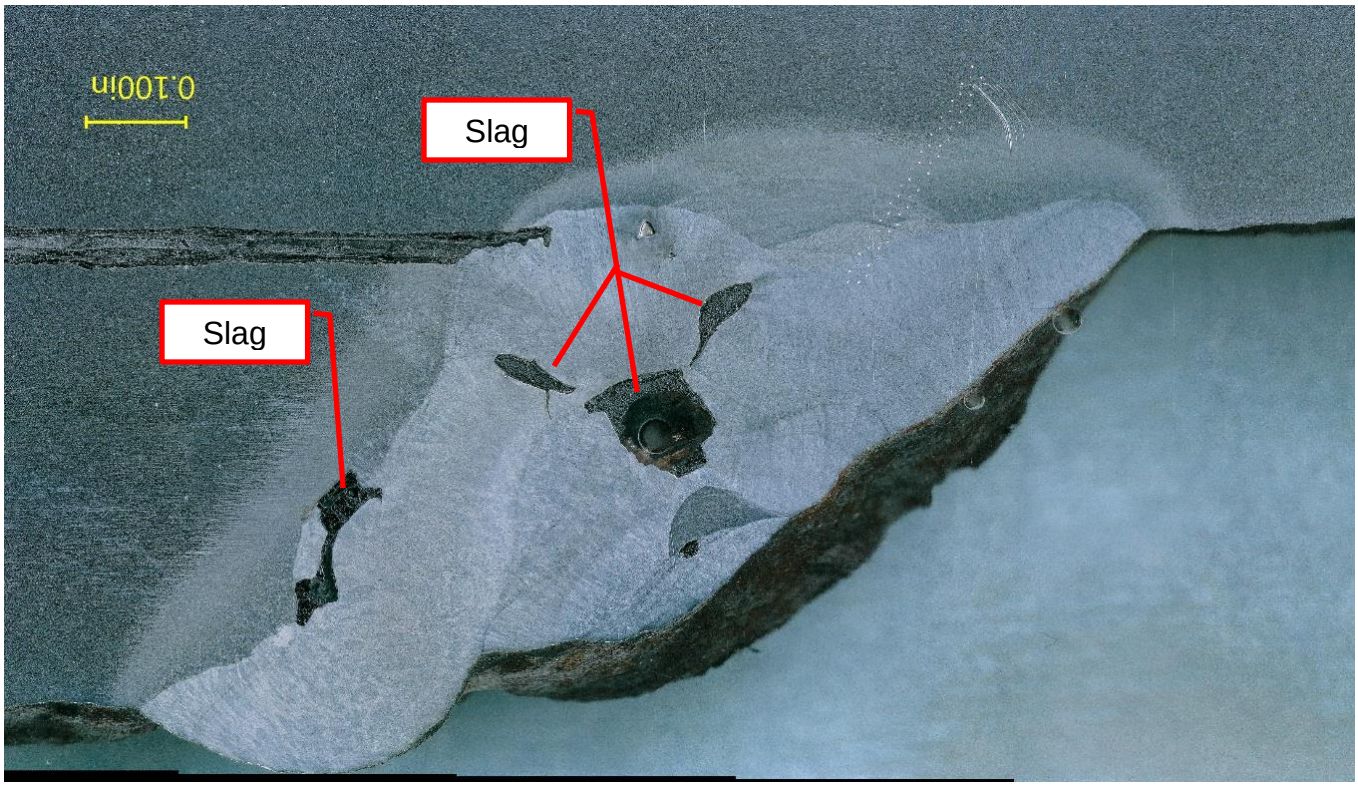

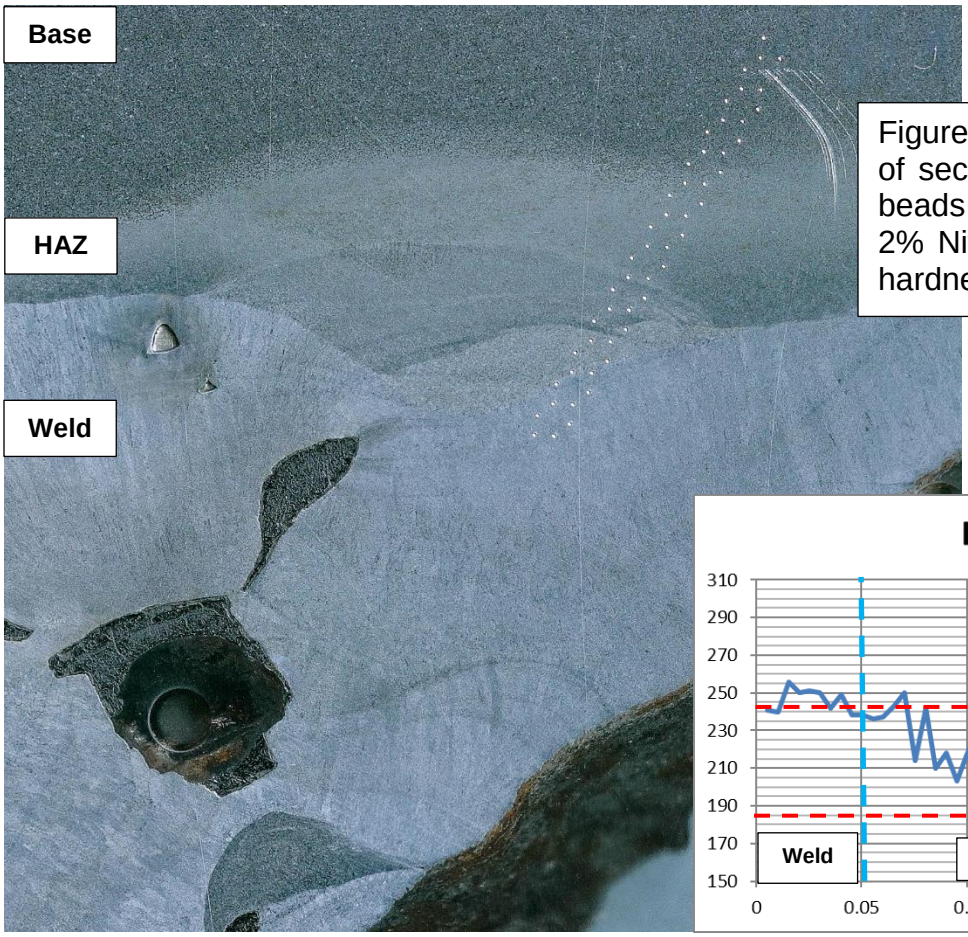

Figure 31. Optical micrographs of section B14 showing multiple beads and large slag inclusions. 2% Nital etch. Graph of Vickers hardness, traverse below.

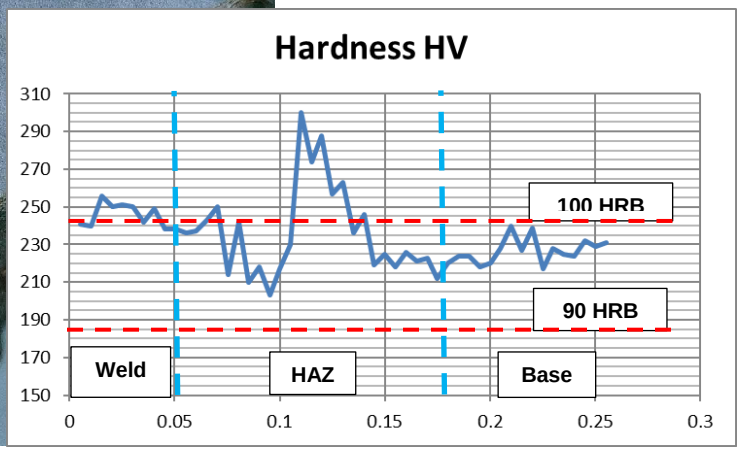

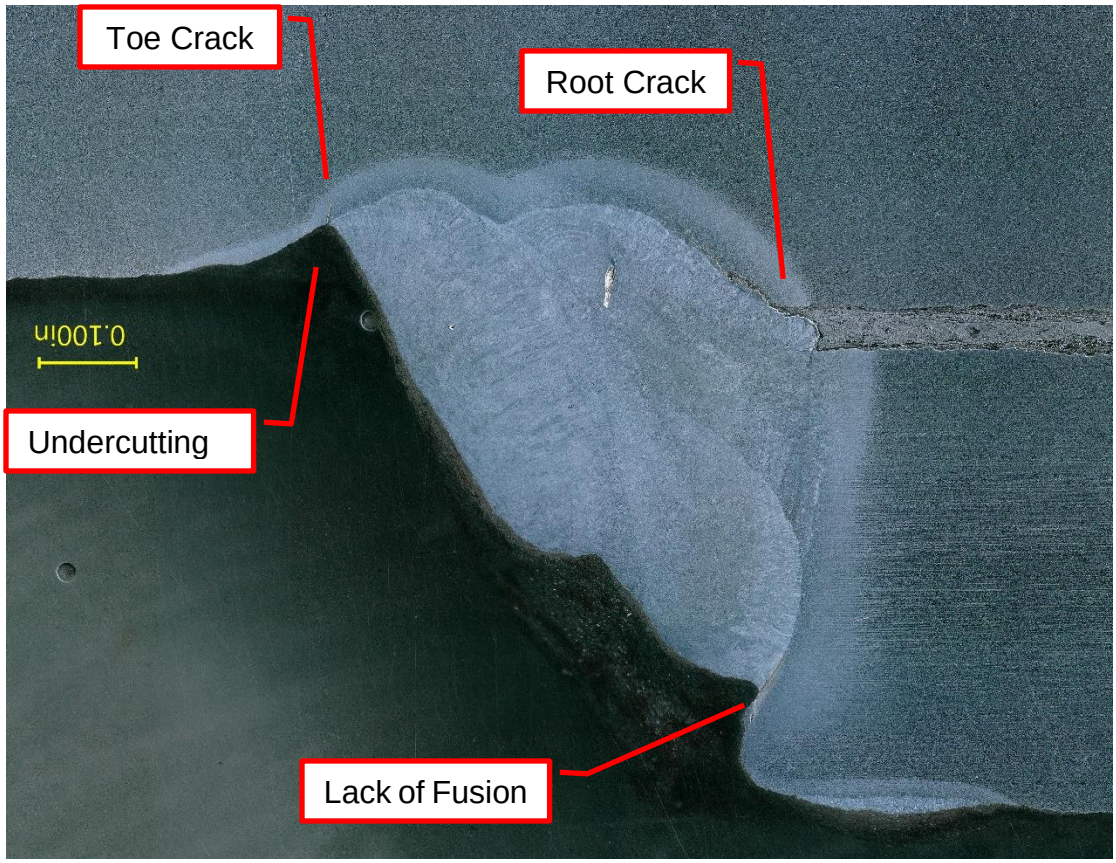

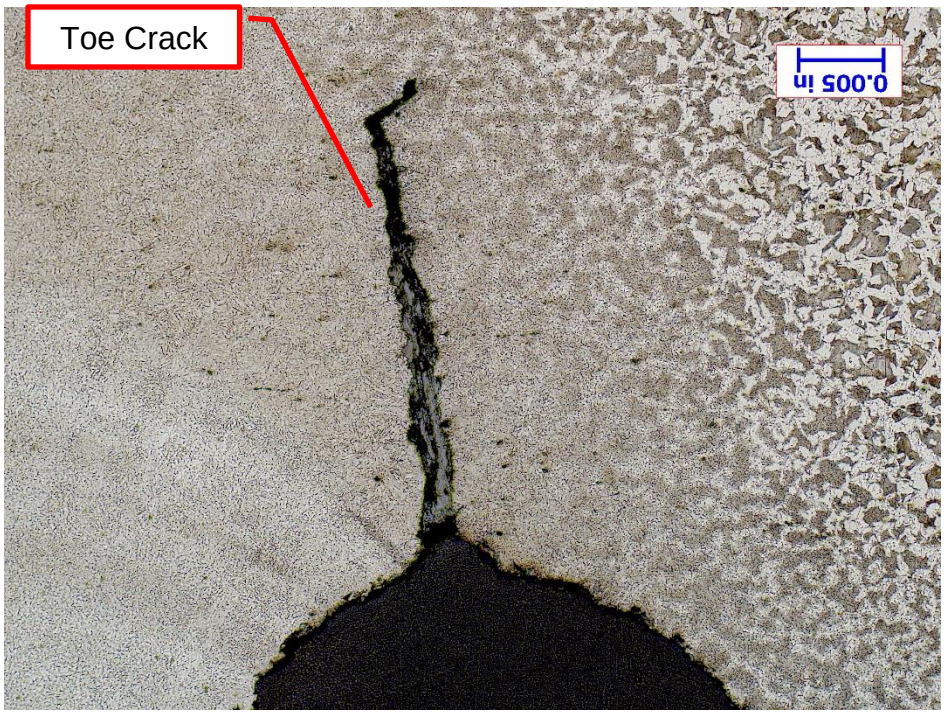

Figure 32. An overall micrograph, top, of section B15 showing the locations of the toe and root cracks and the areas of undercutting and lack of fusion. The toe crack is shown at greater magnification at left. Root crack and lack of fusion are shown in figure 33.
2% Nital Etch

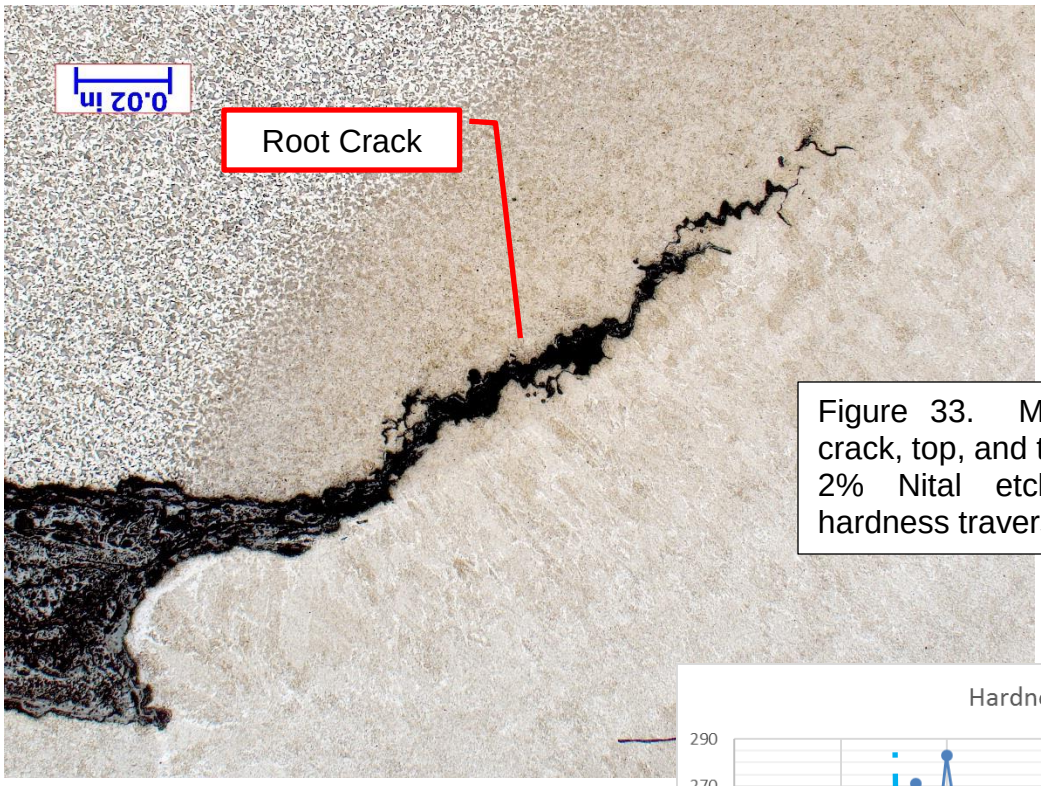

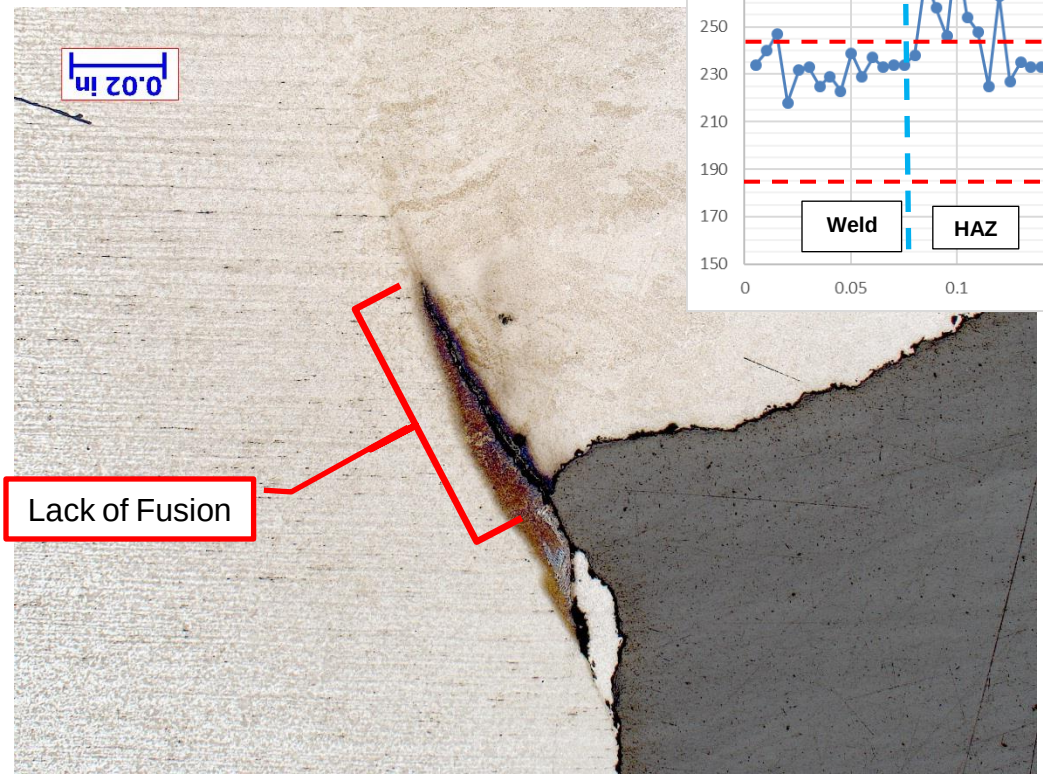

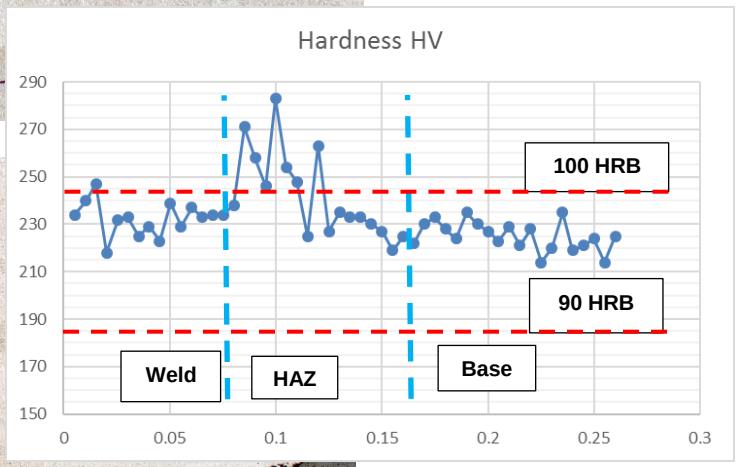

Figure 33. Micrographs of the root crack, top, and the lack of fusion, below. 2% Nital etch. Graph of Vickers hardness traverse in the middle.

Figure 34. Cut up sections of B end cradle pad weld area with locations and averages of direct HRB hardness measurements.